ENGINEERING RESEARCH INSTITUTE
AIRCRAFT PROPULSION LABORATORY
UNIVERSITY OF MICHIGAN
ANN ARBOR

Final Report

AN ANALYTICAL AND EXPERIMENTAL STUDY OF TRANSIENT AERODYNAMIC PHENOMENA AND RELATED EFFECTS IN THE RAMJET ADDITION OF THE ARNOLD ENGINEERING DEVELOPMENT CENTER

HENRY H. HICKS, JR.
ALBERT W. STOHRER
ROBERT L. FITTS

R. B. MORRISON
Supervisor

Project 2122

AIR RESEARCH AND DEVELOPMENT COMMAND
U. S. AIR FORCE
CONTRACT NO. AF 18(600)-547, PROJECT NO. R-741-009

March, 1955

TABLE OF CONTENTS

	Page
LIST OF FIGURES	iii
ABSTRACT	v
OBJECT	vi
SECTION I. GENERAL METHOD OF APPROACH	1
SECTION II. PULSATIONS IN THE EXHAUST SYSTEM	2
SECTION III. WATER-SPRAY ATTENUATION	11
GENERAL INFORMATION	11
SPRAY-DROP SIZES AND DISTRIBUTION	11
AIR-WATER VOLUME RATIO	16
ATTENUATION OF SOUND IN FOG	22
SECTION IV. TESTING OF INDIVIDUAL COMPONENTS	26
SECTION V. THE STARTING CYCLE	35
SECTION VI. APPENDICES	41
Appendix 1. Blade Vibrations	41
Appendix 2. The Sound-Level Meter	43
Appendix 3. Use of the Water Table	44
Appendix 4. Diffraction and the Frensel Integral	47
Appendix 5. List of Symbols	52
SECTION VII. REFERENCES	53

LIST OF FIGURES

		Page
1.	Acoustical circuit of exhauster	5
2.	Development of reverberation formula	5
3.	Spray-head construction	12
4.	Arrangement for sampling water sprays	12
5.	Sample slide used in drop size determination	13
6.	Metallographic camera	13
7.	Spray drops from 0.046-inch nozzle	14
8.	Spray drops from 0.030-inch nozzle	14
9.	Drop size distribution for two orifice sizes (at constant water pressure)	15
10.	Drop size vs number of drops (constant orifice diameter, variable pressure)	17
11.	Apparatus for measuring sound attenuation	17
12.	Vane anemometer	18
13.	Calibration curve for vane-type anemometer (vane, 2.75" x 6.0")	19
14.	Apparatus for vertical measurement of sound attenuation	21
15.	Attenuation vs frequency, horizontal spray test	23
16.	Scale model, ramjet addition (20:1)	27
17.	Photograph of ramjet-addition model	28
18.	Experimental apparatus for determining the characteristics of ducting components	29
19.	Standing wave traverse at 500 cycles (square corner without turning vanes)	31

LIST OF FIGURES
(continued)

		Page
20.	Mitered corner with turning vanes	33
21.	Reflection coefficient vs frequency	33
22.	Idealized, feed-around circuit	36
23.	Idealized, feed-around circuit	37
24.	Idealized, corner-reflection coefficient	38
25.	Water table assembled for wave study	45
26.	Geometrical construction for diffraction analysis	47
27.	Wave intensity behind a straight edge	50
28.	Spiral of Cornu	51

ABSTRACT

The aims of the project which are the subject of this report have been considerably modified since the beginning of the program. Originally, it was thought that an analytical study of certain aspects of the flow transients in the ramjet addition would be sufficient for the needs of the designers. Subsequent developments showed that the emphasis of the work should be placed on the exhauster system and as this work progressed, it became apparent that the most urgent problem involved the interaction between an engine under test and the exhauster equipment. An approximate method for determining this relation has been developed, and the method of solution is based on data and concepts that involve many other aspects of the system.

OBJECT

The general objective of the work which is the subject of this report has been to consider certain aspects of the dynamic operations of the ramjet addition to the Arnold Engineering Development Center. In particular, the objective has been to consider the various forms of dynamic coupling which might exist between the several components of the ramjet addition and to determine what effects these couplings have on the components of the ramjet addition.

SECTION I. GENERAL METHOD OF APPROACH

The ramjet addition of the Arnold Engineering Development Center is arranged in such a way as to raise the possibility that a dynamic coupling may exist between the unit under test and the exhauster compressors.

The coupling may have detrimental effects on the compressors. This situation leads to a problem which involves the behavior of pressure disturbances in a duct system which has water sprays, turns, valves, and water separators, and in which a gas of varying temperature and composition is flowing.

The general complexity of the problem rules out the possibility of the development of a general solution to the problem, but a method of approach capable of giving useful results is developed in Section II of this report. This section is in effect the main part of the report since it is here that the relationship between the unit under test and the exhauster compressor is developed. The analysis in Section II makes use of the water-spray attenuation factor and the corner-reflection coefficient. Since the determination of these factors involved a considerable amount of work and some unusual concepts, they have been considered in Sections III and IV of the report. These sections are intended to support Section II. Section V is an independent part although it makes use of the corner-reflection coefficient of Section IV. Section V is included to cover the additional work which was done to investigate the starting conditions in the ramjet addition. The main purpose of this work was to examine the system for possible resonant conditions which could adversely affect the exhauster compressors during the starting cycle.

The appendices of the report are devoted to brief items which are important to the report, but which do not fit conveniently elsewhere. The section on blade vibration contains material used directly in Section II. The discussion of the sound-level meter is included because it was the main measuring instrument of the study.

At one time, it was believed that the water table would be useful in testing the individual components. This proved disappointing, but the idea still seems to have possibilities; a section on the water table is included. The propagation pattern of waves is predicted on the basis of the diffraction theory, but the pattern of one of the corners with turning vanes is too complex to be practicably analyzed using the diffraction theory. The consideration of simpler cases, however, explains the reflection and transmission characteristics of the individual components; a section is included in the appendices on this subject.

SECTION II. PULSATIONS IN THE EXHAUST SYSTEM

The basic idea which is to be developed in this section is that pressure pulsations which are developed in the exhaust system by the operation of the unit under test may cause harmful effects on the structure of the system or on the exhauster compressors. The most particular danger would appear to come from the effects of a test unit which emitted the steady pulsations characteristic of rough burning and which at times could be in sympathy with certain elements of the compressors. The effects of a single pulse of pressure will also be considered, although the analysis is quite simple in this case.

It should be noted at this time that the objective of this part of the report is to provide a means by which conditions at the compressor, for example, may be computed using known or assumed conditions at the test unit. It is felt that the decision as to whether these conditions are detrimental to the compressor can be best made by the manufacturer of this equipment.

If an arrangement of ducting with elbows, constrictions, enlargements, side chambers, etc., is filled with a gas and the gas is excited into motion at some point by a steady pulsating force, a complex system of pressure and velocity waves will be developed within the contained gas. A complete analytical solution for such a system would define the intensities of the pressure and velocity waves for any and all particular points in the system. The solution would furthermore give the phase relationship for these waves. The difficulty with the analytical approach is in its complexity. Even the solution of fairly simple systems such as a tube with a single restriction placed within involves some rather cumbersome mathematics. A complete analytical solution for a system as complex as the ramjet addition is almost beyond hope. The system is further complicated by a superimposed gas flow, the presence of suspended water droplets, and a changing temperature of the gases in the ducting.

If a complete analytical solution is not practicable, then some approach must be found which will give a meaningful result, and which is not hampered by the rigors of a purely analytical approach. By working with the real part* (as contrasted to the imaginary part) of the complete solution,

*Any general equation relating some quantity (e.g., displacement) of a system to the forcing function causing this displacement will contain real and imaginary terms, provided that the system is made up partly or wholly of reactive elements. In a mechanical system the reactive elements are the mass and the compliance of the system.

the analysis is greatly simplified and practical results can be obtained. Thus, the real acoustical power flow through the system may be computed without need for a detailed knowledge of the pressure pulsation at some point. This approach will provide answers which may be adequate for the problem at hand. This is particularly true since it is the real part of the power flow which provides the energy necessary to maintain destructive vibrations in the system or its components.

The general approach to the solution of a specific case involves the making of assumptions as to the characteristics of and the operating conditions imposed on a particular test unit. The acoustical power flow from the test unit may be computed once these quantities have been assumed or estimated on the best available basis. The effects due to the ducting on attenuating this power flow are then computed, and then the effects on the compressor of the remaining acoustical power are determined.

In order to establish the power flow level due to pulsations in the test unit (engine), a ramjet engine operating at sea level conditions at M-2.0 is assumed as fairly typical. The diameter of the test engine is taken to be 6 feet and the engine exhaust is directly connected to the exhauster system. If the inlet air takes a normal shock on entering the compressor, the static pressure ratio developed is 4.5, and the velocity following the shock is M-0.47. Subsequent subsonic diffusion would increase the static pressure ratio slightly, but the necessity of securing a throughput and minimum cross section for the engine limits the amount of subsonic diffusion that can be utilized. Actual supersonic diffusors which would be used on an engine exceed the 4.50 pressure ratio somewhat, developing about a 6.00 pressure ratio. It could be expected then that the usual combustion chamber pressure with choked outlet would be about 6 atmospheres.

The pulsations that accompany rough burning or "buzzing" in the test engine are apparently due to regenerative instabilities in the combustion process which are related to the pressure variation in some very complex ways. It is thus conceivable that a pressure pulse approaching that due to constant-volume, adiabatic burning could be developed in the engine, giving pressure peaks of the order of 30 atmospheres. A small amount of available information indicates, however, that, pressure pulsations of from 6 to 50 percent of the steady-state pressures have been measured on engines under test. If the higher value is used, then a pressure pulsation of 3 atmospheres may occur in the test engine under some conditions.

The formula for acoustical power in plane waves may be applied now, as follows:

$$I = \frac{p^2 s}{\rho c} \quad ,$$

where

I = acoustical power, ft-lb/sec;
p = rms pressure variation, lb/ft^2;
s = area of duct (cross section), ft^2;
c = celerity of acoustical pressure, ft/sec; and
ρ = average density of fluid, slug/ft^3.

The computed values for the various quantities are:

$p = (0.707)\ (3)\ (14.7)\ (144) = 4480$ lb/ft^2 [for sinusoidal wave],
$s = \pi/4(6^2) = 28.3$ ft^2,
$c = 2170$ ft/sec (for temperature of 1500°F), and
$\rho = 0.0038$ slug/ft^3 (6 atmospheres steady-state pressure).

The resulting acoustical power generated is therefore:

$I = 69 \times 10^6$ ft-lb/sec $= 125{,}000$ hp.

This is a rather surprising amount of power to be associated with the pulsating energy, but a ramjet engine of the assumed size would develop about 500,000 equivalent horsepower at operating speed, and the result is not unreasonable on this basis. The ramjet engine applies this acoustical power completely to the exhauster system since the two are directly connected.

It is now necessary to consider the effect of the ducting system on the power that is being fed into it. This would be exceedingly difficult if it were not for the presence of the water spray which imposes a very large attenuation on the pulsating power. The analysis to be used here is typical of the approach used in reverberation studies where the build-up of energy in rooms is considered under the influence of a constant imput power.

The part of the acoustical circuit of the exhauster system under consideration is shown in Fig. 1. Considering Fig. 1, it is assumed that the power flow from the engine is unity in the beginning. After one pass through the water spray, the intensity is reduced to α. At the first corner, the power reflected back is $\alpha\beta$ and the amount sent on around is $\alpha(1-\beta)$. When the reflected power reaches the engine there has been another attenuation factor, α, applied which now brings the intensity to $\alpha^2\beta$. The reflection coefficient, γ, at the engine returns the quantity $\alpha^2\beta\gamma$ to the ducting.

This continuing process is outlined in the diagram shown in Fig. 2. The net transmitted power from the system is the sum of the columns between headings B and C. Some power is reflected from corner C and returns to the region A-B to modify the situation there, but because of the large effect of α, this can be practically neglected. It is further assumed here that there is not much water left in suspension after the first corner has been passed.

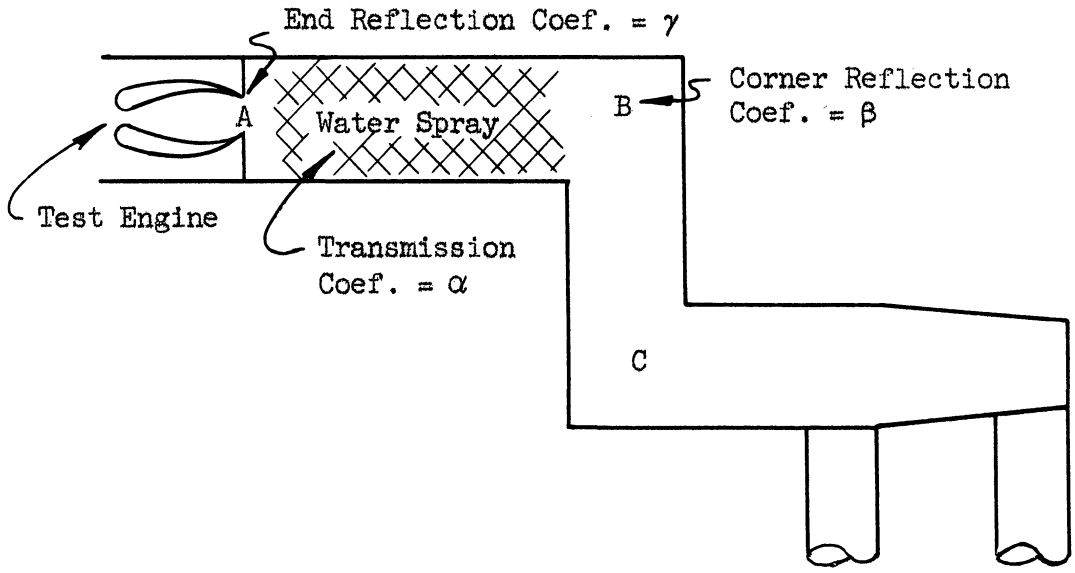


Fig. 1. Acoustical circuit of exhauster.

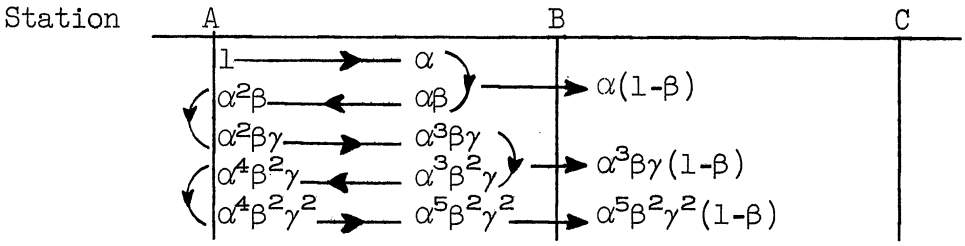


Fig. 2. Development of reverberation formula.

The net transmitted power is then reducible to an infinite series which converges to the sum:

$$I_t = (1-\beta)\left[\alpha\left(1 + \frac{1}{1-\alpha^2\beta\gamma}\right)\right] .$$

The values for the constants in the reverberation formula may now be evaluated. α is the attenuation coefficient due to the water spray and from the experimental and analytical work in the water-spray section, a power loss of 10 decibels per pass can be expected. This sets the value for α to be 0.10. The value for the corner-reflection coefficient taken from the section on individual components is 0.80. The reflection coefficient γ is determined by the impedance mismatch at the sudden contraction on entering the tailpipe of the engine. The analogous acoustical impedances at this point are inversely proportional to the areas of the ducting and of the engine tailpipe. If the area of the tailpipe is termed A_1 and the area of the adjoining ducting termed A_2, then the analogous impedences are proportional to $1/A_1$ and $1/A_2$.

The ratio between the reflected power and the incident power is then given by:

$$\frac{I_r}{I_i} = \left(\frac{\frac{1}{A_2} - \frac{1}{A_1}}{\frac{1}{A_2} + \frac{1}{A_1}} \right)^2$$

Noting that areas of circular ducts are proportional to diameters squared:

$$\frac{I_r}{I_i} = \left[\frac{\left(\frac{1}{D_2}\right)^2 - \left(\frac{1}{D_1}\right)^2}{\left(\frac{1}{D_2}\right)^2 + \left(\frac{1}{D_1}\right)^2} \right]^2 ,$$

and since

$D_1 = 6$ ft, $\quad D_1^2 = 36$ ft^2, and $\quad \frac{I_r}{I_i} = \gamma = 0.56.$
$D_2 = 16$ ft, $\quad D_2^2 = 256$ ft^2,

In summation for this particular problem:

$\alpha = 0.10,$
$\beta = 0.80,$ and
$\gamma = 0.56.$

By applying the reverberation formula, the net fraction of transmitted power becomes:

$I_t = 0.04$ of the generated power,

and since

I generated = 125,000 hp,

$I_t = 5{,}000$ hp.

This power is then transmitted without great loss through the remainder of the ducting system and into the compressor. As mentioned earlier, no information is given by this analysis as to the pressure pulsation level existing at any particular point in the system. It can be said, however, that conditions must adjust themselves so that the waves traveling in opposite directions are of such amplitude that the power flow requirement is satisfied.

In order to determine the effect of the transmitted power on the compressor, it is necessary to exercise some judgment concerning the blading

arrangement. Here again a complete analysis is impractical owing to the general complexities of the arrangement, but considering the first row of blades in the compressor, a good approximation of the power applied can be based on the catch area for the blades. On this basis, the power applied to the second row of blades is determined by the catch area of this row and the portion of the power unextracted by the first row.

Actual dimensional data are not immediately available for the first row of blades which is the guide vane, but it is assumed that the blades are similar in construction to the second row of blades (the first-stage rotor blades). On this basis, the projected catch area for one guide vane is 36 square inches. The total annular compressor inlet area at the guide vane is 9,580 square inches. There are 78 guide vanes. These additional data are used with previous calculations to obtain the power input to the guide vanes.

For each guide vane, this turns out to be 18.8 hp and the power applied to all the guide vanes is 1,470 hp. This leaves 3,530 hp which passes into the second row of blades (the first-stage rotor). Similar calculations show that each first-stage rotor blade receives 13.3 hp of acoustical energy. Succeeding blade rows are computed in the same manner.

The next step in the computation is to determine the effects of the applied power on the row of blades under consideration. This applied acoustical power must correspond to the resonant frequency of the blades (otherwise they will not absorb energy readily) and for this reason a considerable restriction is placed on the possible causes of damage.

The amplitude of vibration of individual blades is determined by the power input to the blade, the spring constant of the blade, the logarithmic decrement, and the frequency of vibration of the blade.

The method of computing the amplitude of blade vibration is straightforward, and is not included in this section. The results of the computation give the amplitude of the guide vanes to be 1.41 inches and the amplitude of the first-stage rotor blades to be 1.82 inches. These are tip amplitudes and the direction of motion is the same as that used by the manufacturer in determining the spring constants and damping factors for the blades.

Considering the length of the blades, the amplitudes calculated seem too large to be safely handled, but it is felt that this decision can best be made by the manufacturer of the compressor. It may properly be questioned whether the size of the ramjet engine that was chosen was really representative of the maximum size to be tested, and perhaps the assumed operating conditions were too severe. These factors can be easily adjusted on the basis of more complete information, but once the operating conditions have been chosen, the analysis leads to definite results which must be taken into account.

There are other factors which can influence the results to some extent. For instance, it was assumed that once the acoustical power flow had left the spray chamber, there would be no further losses on this power until it reached the compressor. This is, of course, not exactly true. Some power is applied to the ducting itself. When the tests were made on the model components, the losses noted were so low that they could not be readily distinguished from the inherent instrumentation errors. For this reason the conclusion is that a large portion of the calculated energy will reach the compressor blades.

The exact calculation of the amount of energy in a sharp pulse is usually difficult, and a graphical analysis is used. There is no general formula for calculating the energy in a pulse, since this quantity depends on the shape of the pulse. Roughly, the energy in a sharp pulse may be quickly calculated by comparing the energy in the pulse to that in a single fluctuation of a steady wave. The frequency of the steady wave used for comparison must be estimated, based on the sharpness of the pulse. If the quantities used earlier in this section are used with a frequency of 300 cycles per second, the energy for pulsation is

$$E = \frac{69 \times 10^6}{600} = 1.15 \times 10^5 \text{ ft-lb.}$$

No reverberation can build up with a single pulse, so the portion of this energy which reaches the compressor depends on the successive transmission coefficients of the elements in the line. These are three corners and the water separator.

Using the energy transmission coefficient of 0.50 for each of these elements, the total transmission coefficient becomes 0.0625. The energy which reaches the compressor is then

$$E = 1.15 \times 10^5 \times 0.0625 = 7.20 \times 10^3 \text{ ft-lb.}$$

Of this energy, the amount which reaches one guide vane, for instance, is

$$E = \frac{7.20 \times 10^3 \times 36}{9580} = 27.0 \text{ ft-lb.}$$

Of this energy, only a part is transmitted to the blade owing to the large differences in the specific impedences of the blade and the air. This quantity is ρ_c and these values are for:

air = 2.04 and
steel = 64,000.

$$\text{Reflection fractions} = \left(\frac{64{,}000 - 2.64}{64{,}000 + 2.64}\right)^2 = 0.999 \ .$$

This leaves only about 0.027 ft-lb of energy of the original pulse which is applied to the blade. This quantity is apparently entirely negligible.

In this section of the report, a method of relating pressure changes in the test chamber to their effect on the compressor blading has been developed. Two conditions have been considered; the steady pulsation and the pulse. Of these two conditions, the steady puslation appears to be the only one capable of affecting the system adversely.

The analysis is based on the real power concept of wave motion. This simplifies the problem enough so that it is at least manageable, although certain useful information is lost in the process.

The final form of the connecting relation is developed on page 5 of the report and is

$$I_t = (1-\beta)\left[\alpha\left(1 + \frac{1}{1-\alpha^2\beta\gamma}\right)\right]$$

I_t is the portion of acoustical power applied to the exhauster system that finally reaches the compressor. This relationship is based on the assumption that it is only the water spray which attenuates the sound pulsations. The corners and the water separator may reflect and transmit pressure pulsations, but do not account for much energy loss.

It is realized that the corners, etc., must account for some energy loss, but this loss could not be detected on the model apparatus, and the losses on the full-scale equipment may be even smaller.

In order to make the analysis less abstract, a numerical example was chosen to illustrate the method of approach. The quantities were chosen for this example on the basis that they represented something near maximum conditions to be expected. The nature of the propulsive unit under test is not important; it is the level of pressure pulsations produced that matters, and regardless of the level of these pulsations, the application of the method described is the same.

It was mentioned above that the use of the real power concept resulted in the loss of certain useful information. For instance, the conditions calculated can be expected to occur at only certain combinations of operating conditions that involve pulsation frequency and exhaust gas tempera-

ture, velocity, and composition. It is by no means certain that all of these conditions will be realized during any particular run, and the real power analysis gives no information about these matters. It can only be stated that the possibility of the simultaneous occurrence of all the necessary conditions does exist.

The real power analysis does not directly give any information concerning standing pressures at points along the exhauster ducting, and this is its greatest weakness since this information, if available, would allow the computation of the power lost to the walls of the ducting, etc. It is believed that this power loss is significant, but since it cannot yet be computed or estimated, it cannot be subtracted from that power applied to the compressor blading. The net result of this situation is that the stresses calculated for the compressor blading will be somewhat too high.

SECTION III. WATER-SPRAY ATTENUATION

GENERAL INFORMATION

The water-spray attenuation factor "α" is introduced and used in Section II. The purpose of Section III is to show how the above factor is analytically or experimentally evaluated. This has proved to be a difficult subject in both the foregoing respects, but a substantial amount of progress has been made.

Considering the experimental part of the investigation, it has been necessary to develop equipment and techniques for the purpose. The chief factors to be determined experimentally are spray-drop sizes and distribution, air-water volume ratios for given spray applications, and the attenuation of pressure (sound waves due to the spray). The obstacles to making precise measurements of the experimental quantities have not been fully overcome.

SPRAY-DROP SIZES AND DISTRIBUTION

In order to provide a correlation between experimental and analytical approaches to the attenuation determination, it is necessary to know the effective drop sizes being used. Spray characteristics for two spray heads (Fig. 3) were determined. The general arrangement of the apparatus used for these tests is shown in Fig. 4. The experimental technique consisted of recording the water flow rate through the rotameter and the nozzle pressure as indicated by a Bourdon tube gauge. At the same time a sample of the spray was collected on a specially prepared glass slide. The preparation given the slide consists of a coating of an oil of approximately the same density as water, and then covering the oil with a film of a long-chain alcohol which is lighter than water and immiscible in water and oil. The droplets are caught and suspended in the oil layer between the glass and the alcohol. In this way, the droplets retain their spherical shape, and their true size is visible (Fig. 5). The slide is then magnified and photographed with a modified metallographic camera (Fig. 6). The photographs are then registered over a standard grid and the drops are counted according to size. A graph showing the drop count and size distribution for Figs. 7 and 8 is shown in Fig. 9.

It is seen that the larger holes produce only slightly larger drops. In this manner a median drop size and count is determined for the purpose of correlation. The most significant characteristic of the spray head with respect to the properties considered is that the droplet size and distribution

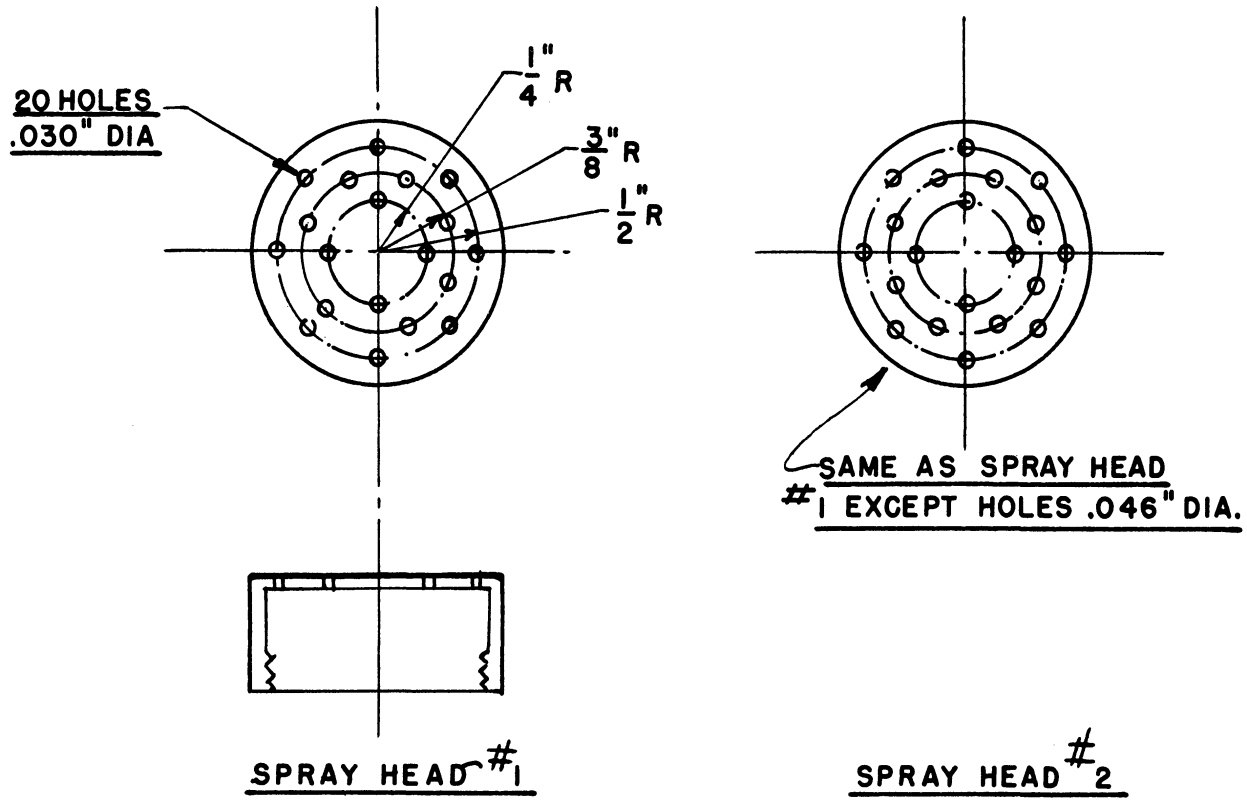


Fig. 3. Spray-head construction.

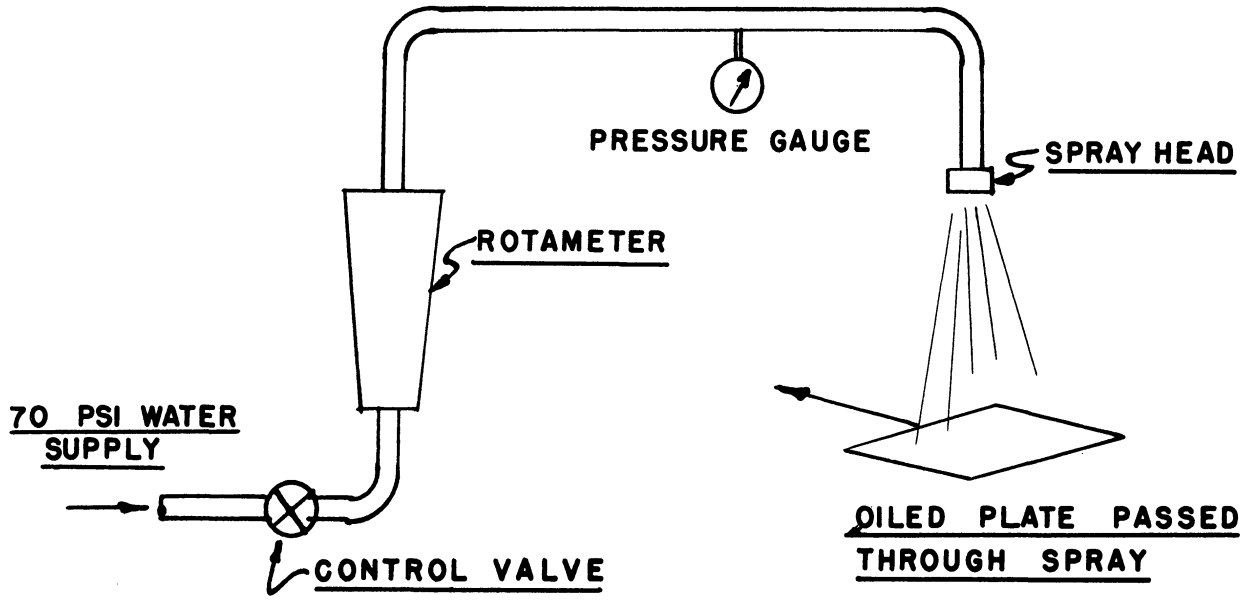


Fig. 4. Arrangement for sampling water sprays.

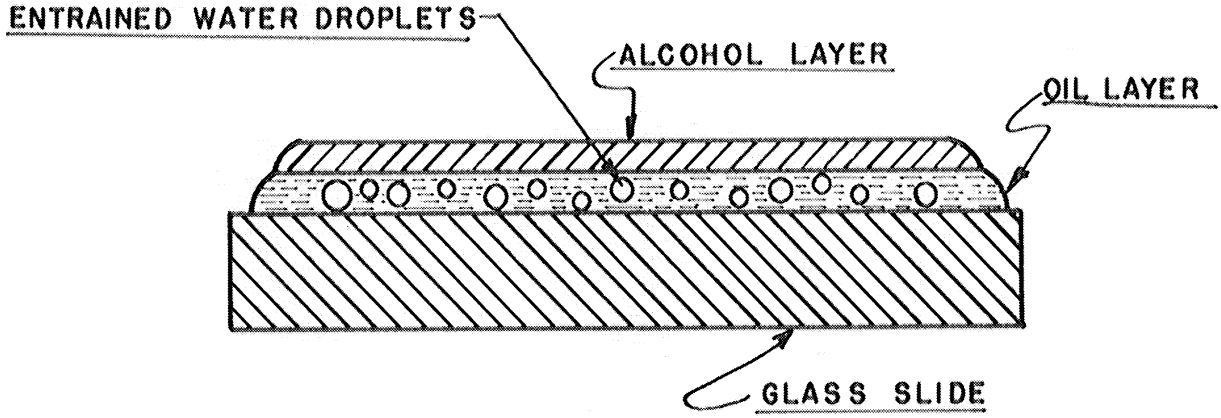


Fig. 5. Sample slide used in drop size determination.

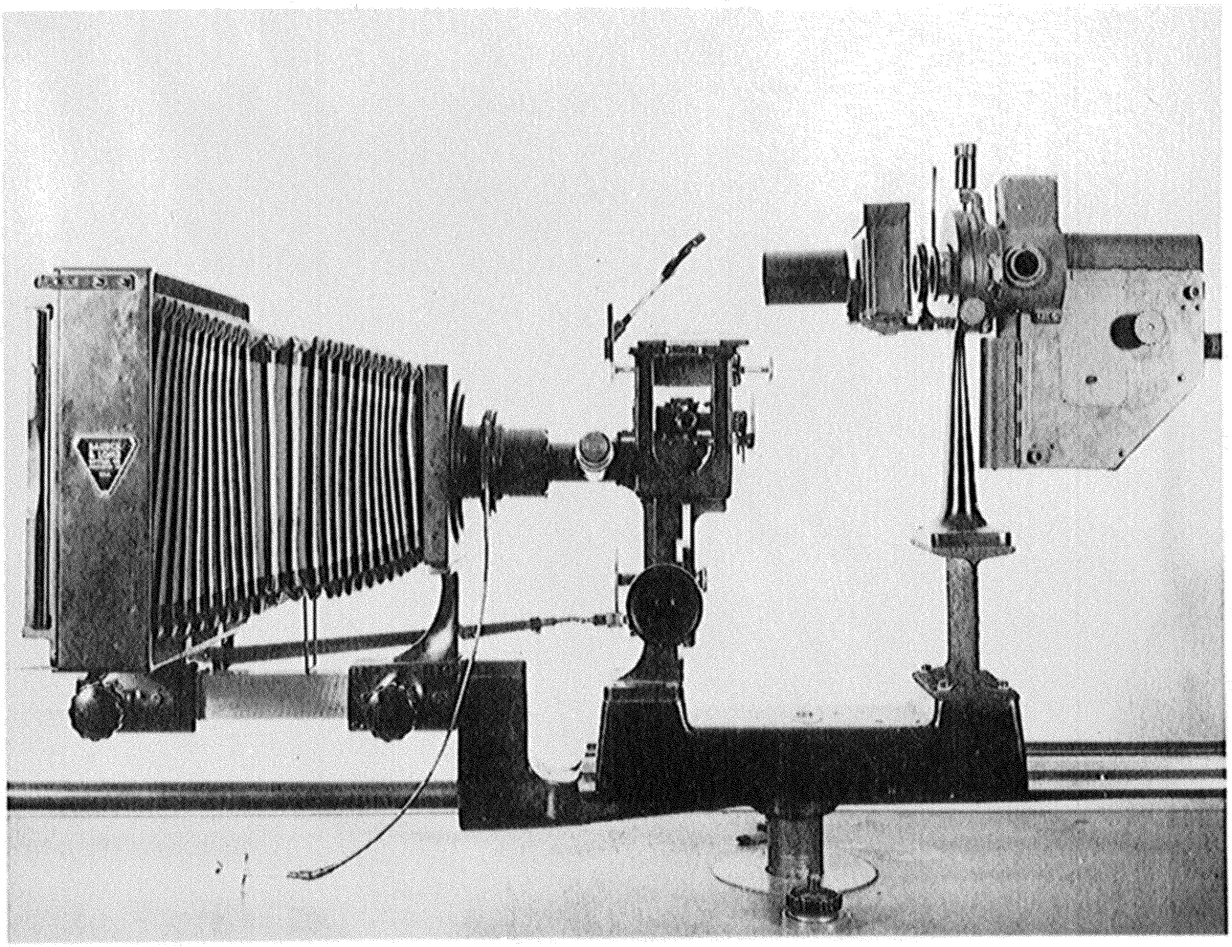
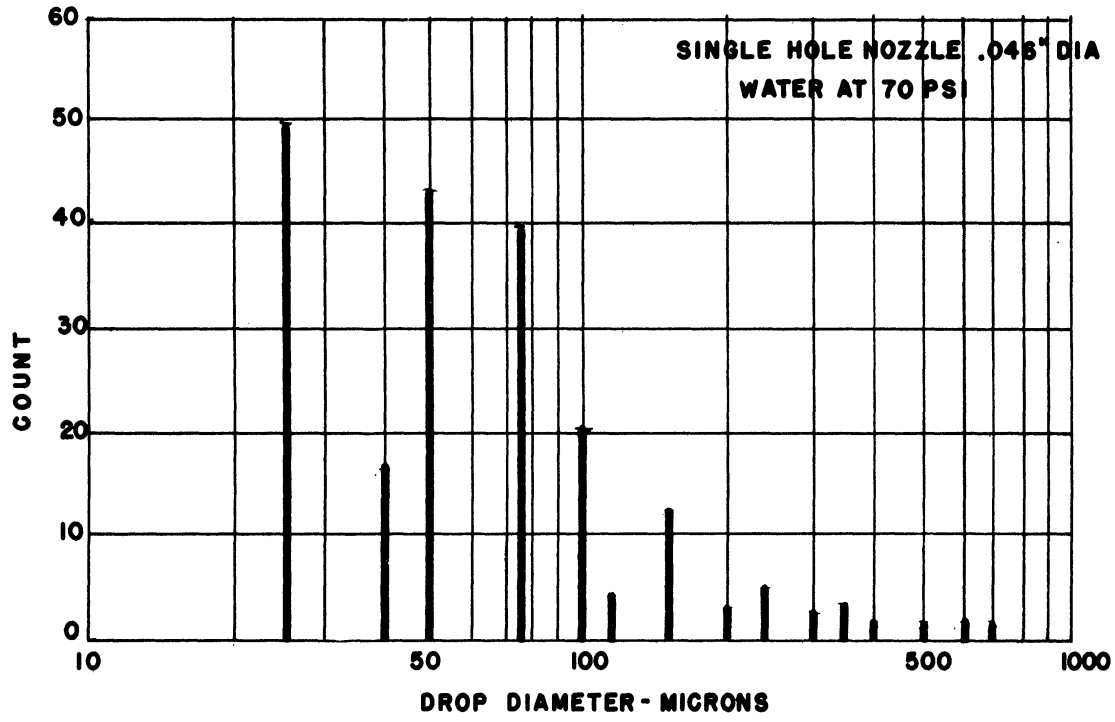


Fig. 6. Metallographic camera.



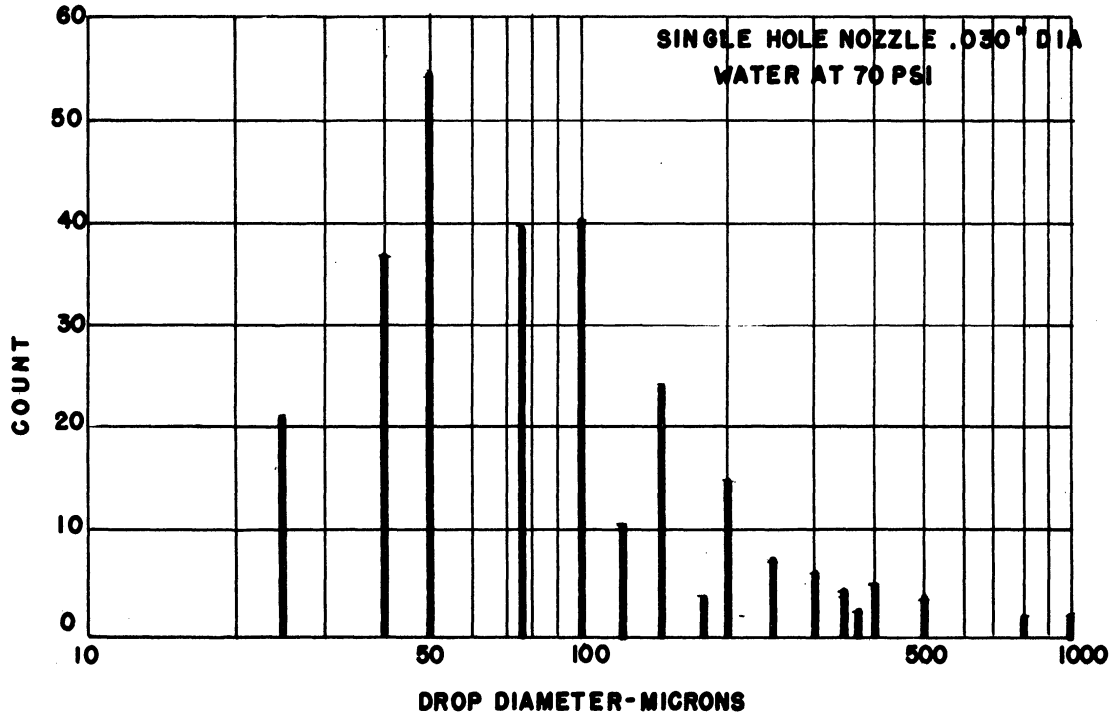
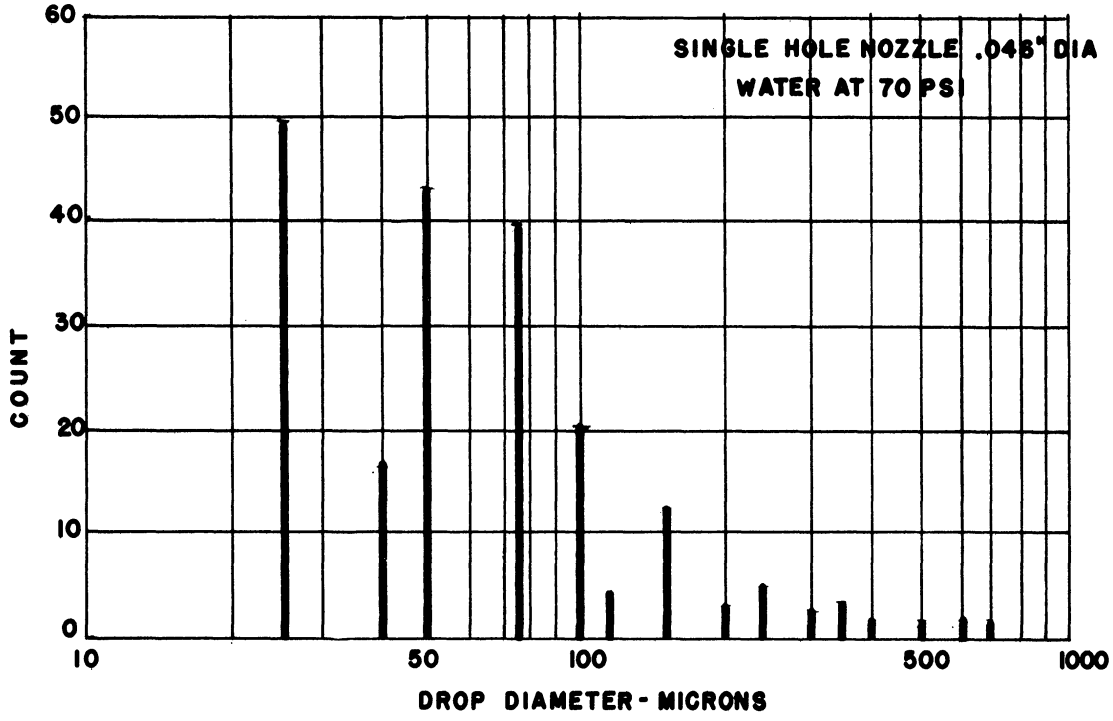


Fig. 9. Drop size distribution for two orifice sizes (at constant water pressure).



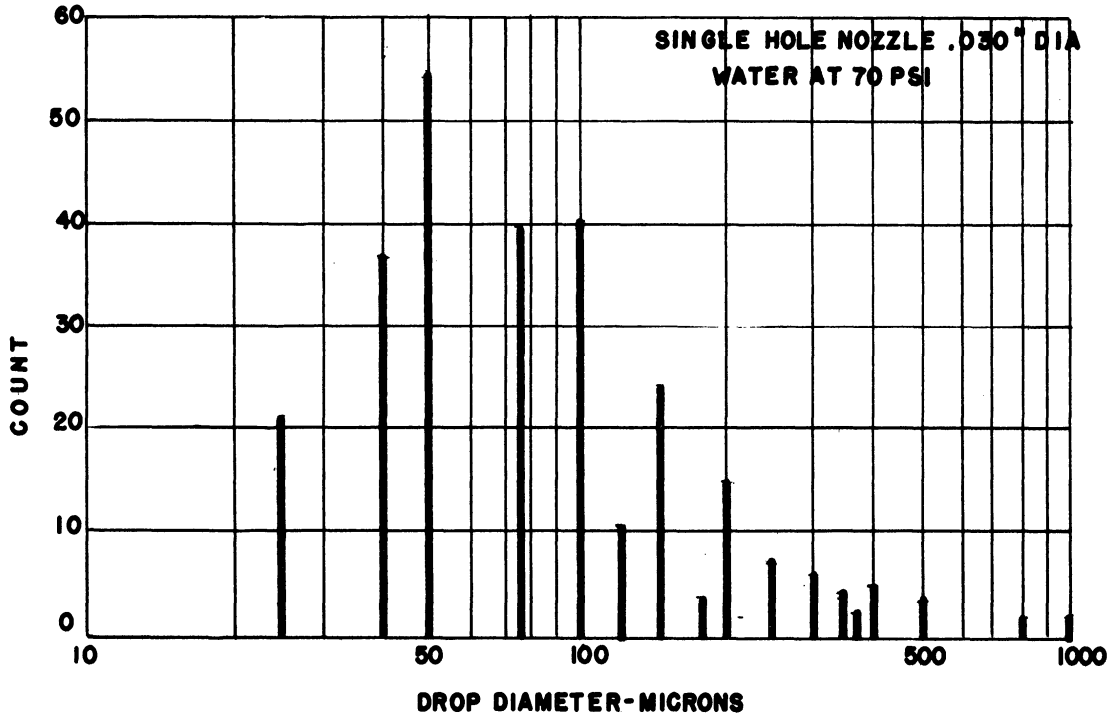


Fig. 9. Drop size distribution for two orifice sizes (at constant water pressure).

is primarily related to the water pressure and not to the diameter of the holes in the spray head. This might be expected on the basis of surface tension requirements necessary to produce sprays, but all spray nozzles produce much larger drops than are predicted from surface-tension considerations.

Although the limiting performance of a spray head can be calculated from surface-tension considerations, the actual performance depends on the distribution of the available fluid energy between surface tension, kinetic energy, induced air, and nozzle friction. No satisfactory method of correlating these variables has ever been found despite a great amount of work which has been done in this country and elsewhere.

The reduction in droplet size distribution for a single spray head with increasing pressure is easily seen in Fig. 10. The graph shows the results of tests made on spray head no. 1. The attenuation resulting from a series of tests made on the horizontal apparatus is shown in Fig. 15. It is noted that the attenuation increases for the high and low frequencies. This variation in attenuation with frequency is predicted from the analytical approaches which have been made. This will be discussed presently.

AIR-WATER VOLUME RATIO

The air-water volume ratio for a given spray depends on the manner in which it is used. In free air, this quantity is determined by the quantity of the spray and by the quantity of air that the spray induces. An analysis of this situation is probably impractical, but in the case of the ramjet addition, it is not necessary to take this approach. The relative quantities of air and water are closely determined by the exhaust system itself and the induced flow should have small effect.

The first experiments to determine the spray attenuation were conducted in a 15-foot length of 10-inch-diameter steel tubing. The tube was placed in a horizontal position and the spray directed into one end of the open tube (Fig. 11). In this case, the water spray induced a flow of air through the tube, but the air velocity was so low that the total head tube could not be used to measure the velocity. An attempt was made to measure the air velocity by adding puffs of various smokes and timing the transit time for the puff. This technique was unsuccessful because the spray washed the smoke out of the air. This particular problem of measuring very low air velocity was resolved by use of a small, vane-type anemometer made for the application (Fig. 12). This device was calibrated by placing it at various positions on a rotating arm in still air. The rounds per minute of the arm could also be varied. In this manner, the speed of the device relative to still air could be computed, and by noting the deflection angle of the vane, a calibration chart for the device could be prepared (Fig. 13). It turned out that the horizontal setup of Fig. 11 was inadequate for several reasons. The most important

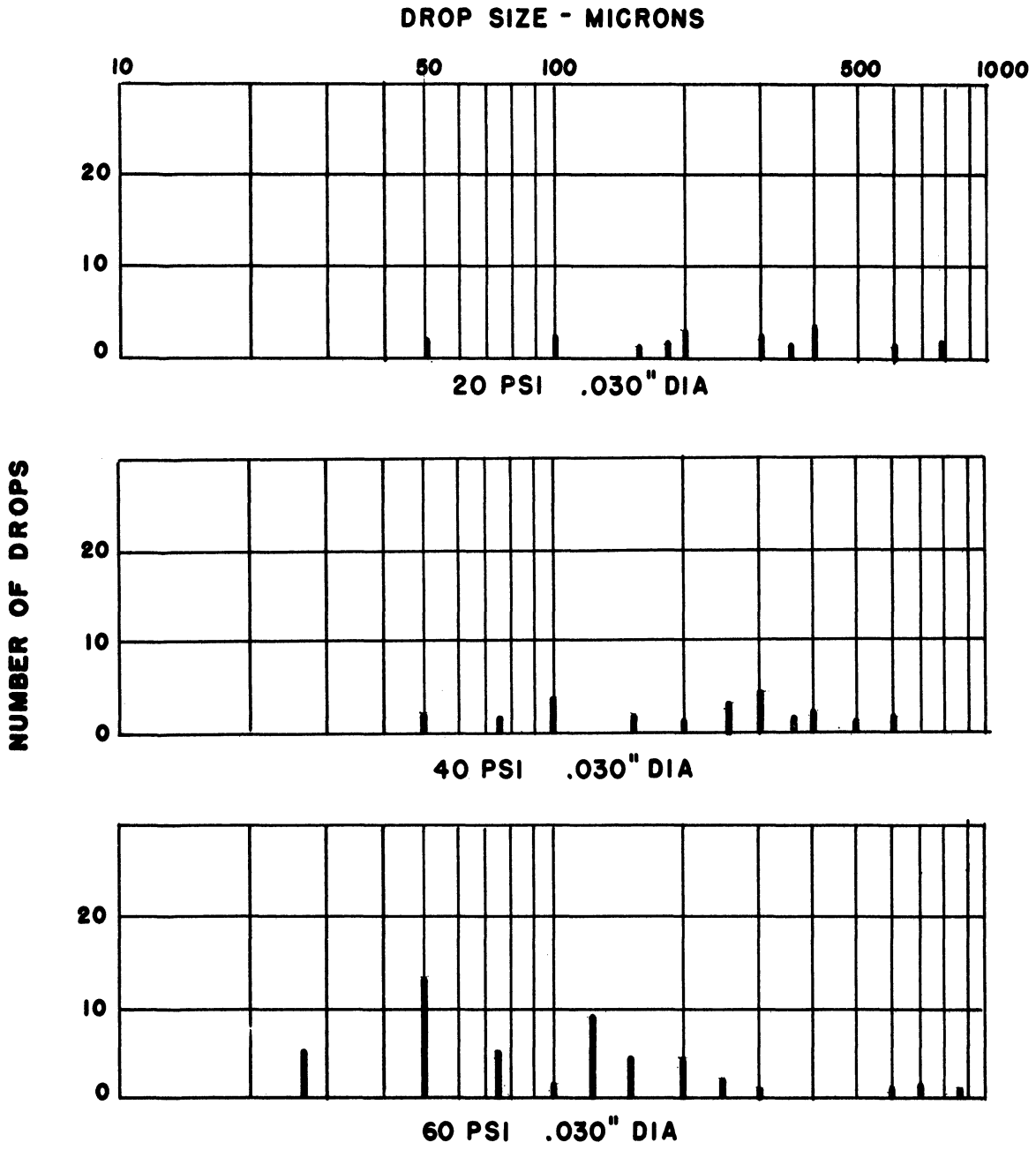


Fig. 10. Drop size vs number of drops (constant orifice diameter, variable pressure).

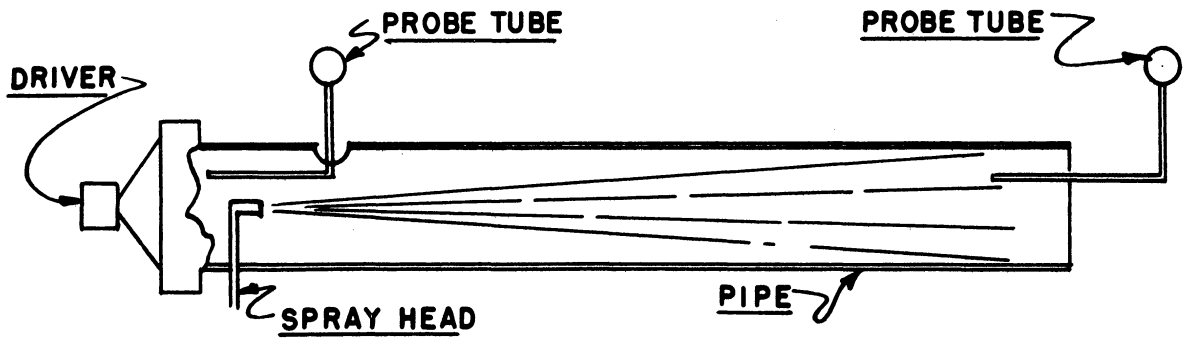


Fig. 11. Apparatus for measuring sound attenuation.

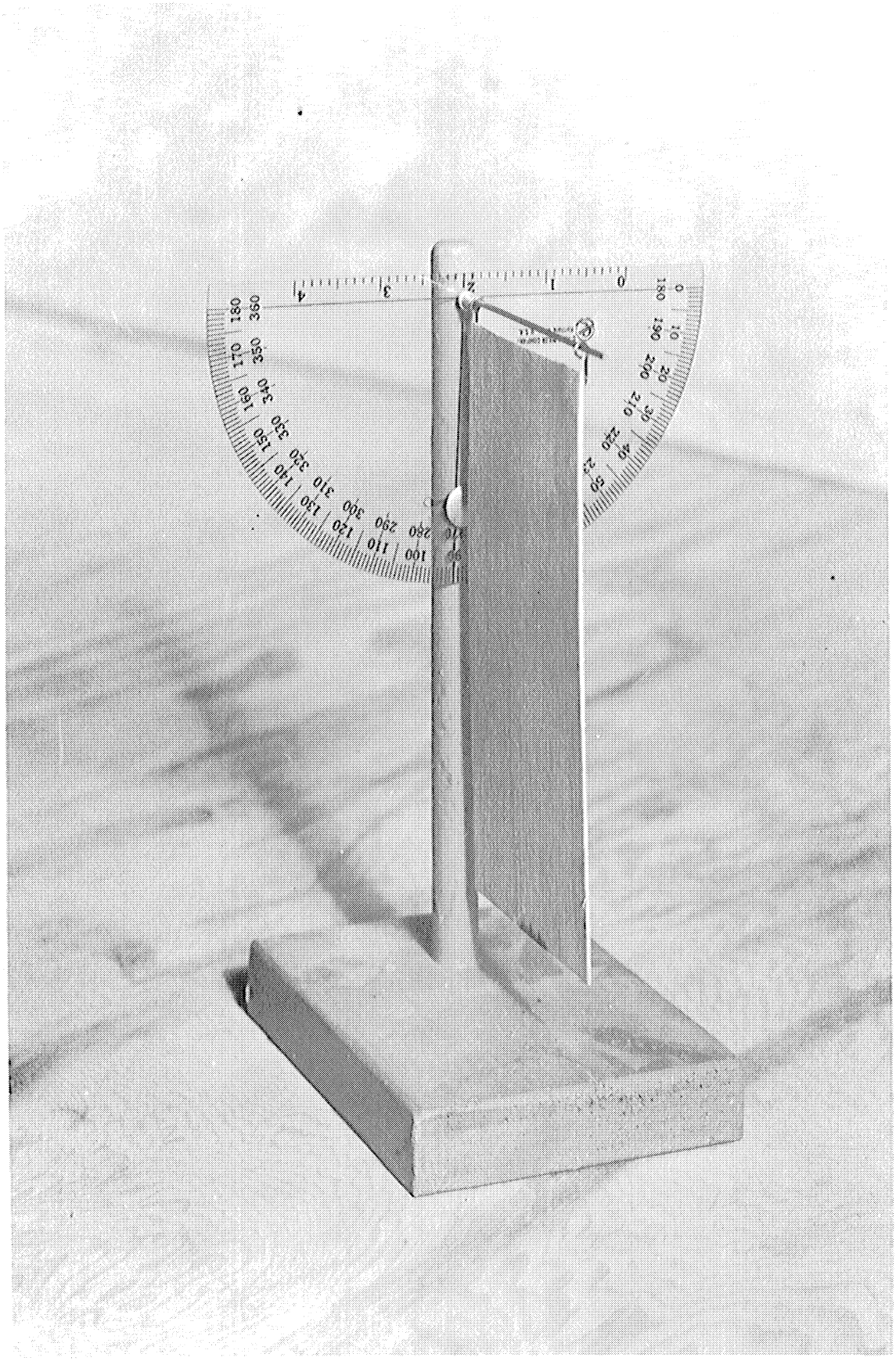


Fig. 12. Vane anemometer.

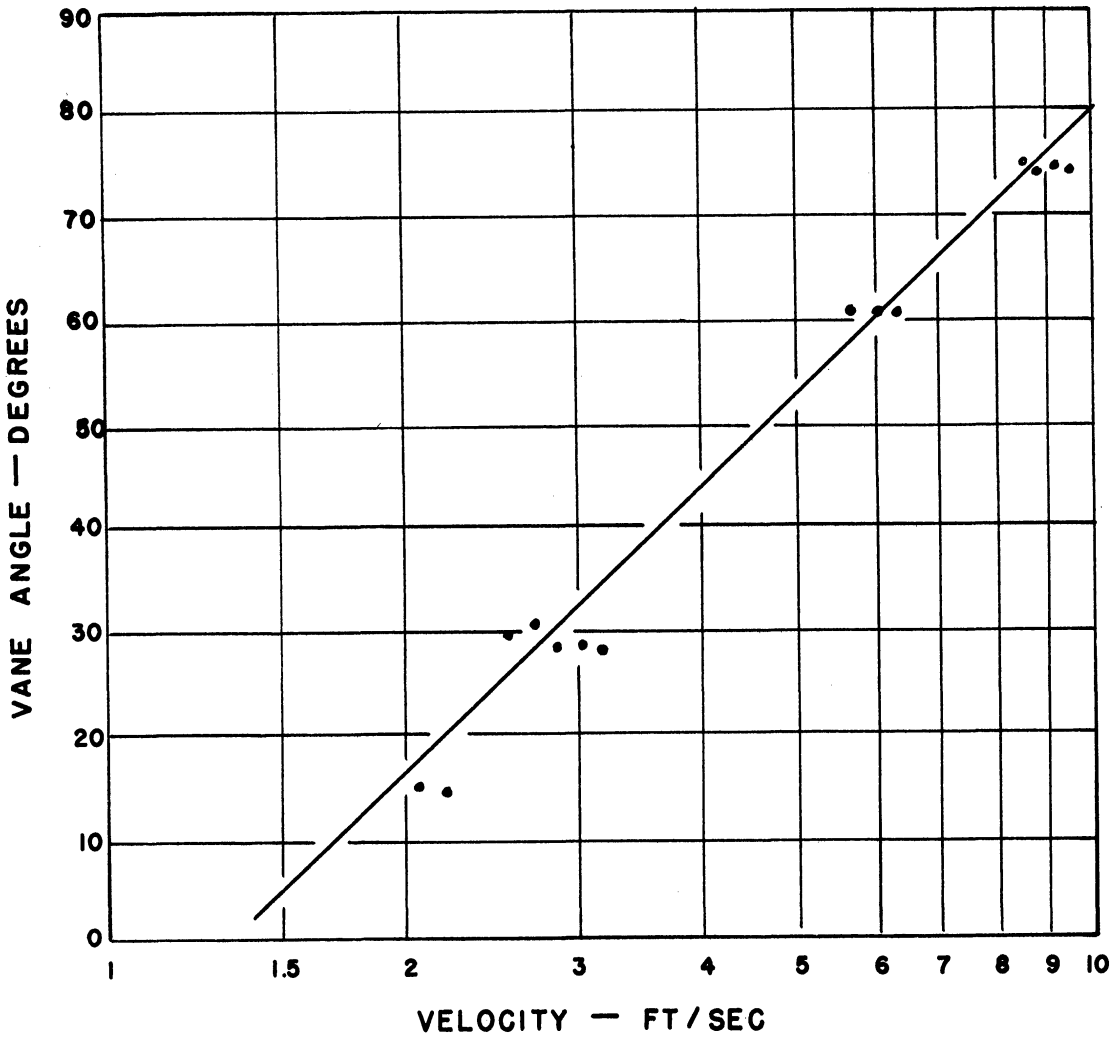


Fig. 13. Calibration curve for vane-type anemometer (vane, 2.75" x 6.0").

of these was the lack of a proper termination for the tube. This is important because unless the tube is terminated properly (analogous to nonreflective termination in an electrical transmission line) standing waves will exist in the tube. The usual technique of terminating such a tube is to fill the end of the tube with a material that is highly absorbent to sound. This technique did not work here because the tube being in a horizontal position provided poor drainage for the packing material which filled up with water and no longer provided an effective termination. The standing waves cause difficulty because the position of the sound-level pickup relative to the nodes and antinodes is very critical. Even if the position of the pickup is rigidly fixed, the introduction of the spray into the duct alters the velocity of sound slightly (due to the humidity change and the drops present) and this changes the end conditions slightly. The only way to accurately determine the attenuation when standing waves are present is to traverse the entire length of the tube with a pickup device and plot the intensities of the pressure antinodes

as the pickup traverses the tube. This could not be done because the probe tube could not be made long enough (because of losses in the probe tube) to traverse a representative length of the spray tube. A waterproof microphone might have been used but was not available at this time.

Another difficulty with the horizontal arrangement resulted from the "fall out" of the spray in the tube so that it was difficult to determine the actual volume of the tube which was filled with spray. The vane anemometer, while quite useful for measuring low air velocities, was erratic because of the impingement of water droplets on its surface. Considering these difficulties it was decided to rearrange the setup so that the tube was placed in a vertical position (Fig. 14). In this case, the "fall out" from the spray was not such a problem, and the packing material was in a position to drain properly so that the standing waves could be reduced.

Furthermore, the air in the tube was nearly stagnant under these conditions and the problem of calculating air-water volume ratios was greatly simplified. A small carbon-button microphone was obtained and waterproofed in a suitable manner. This microphone was lowered into the tube through the spray to determine the attenuation as related to tube length.

One major difficulty in making the attenuation measurements in this manner comes from the noise generated by the spray itself which tends to mask the sound introduced into the tube. Certain frequencies of the noise spectrum will be favored because of resonance in the tube. This difficulty can be partly resolved by using a sound which does not correspond to a resonant frequency of the tube and by using tuned filters in the microphone line to discriminate against the noise.

Unfortunately, the latter series of experiments was terminated by the fire which destroyed the building and the water-spray testing equipment. The work in progress at the time of the fire was aimed at getting a nonreflective termination in the tube. This is a cut-and-try process, and considerable manipulation of packing materials must be done. Some attenuation data were taken during this period, but it is of doubtful value since the primary objective was to get the equipment in proper working order.

Returning to the work done in the horizontal test setup, a calculation based on analysis using the known conditions applied to the test has been using the following conditions:

diameter of duct = 10 in.,
length of duct = 15 ft,
water flow rate = 5 gal/min,
median drop size = 50 microns,
air flow rate = assumed 0 ft/sec,
sound frequency = 300 cycles/sec, and
nozzle drop velocity = 100 ft/sec.

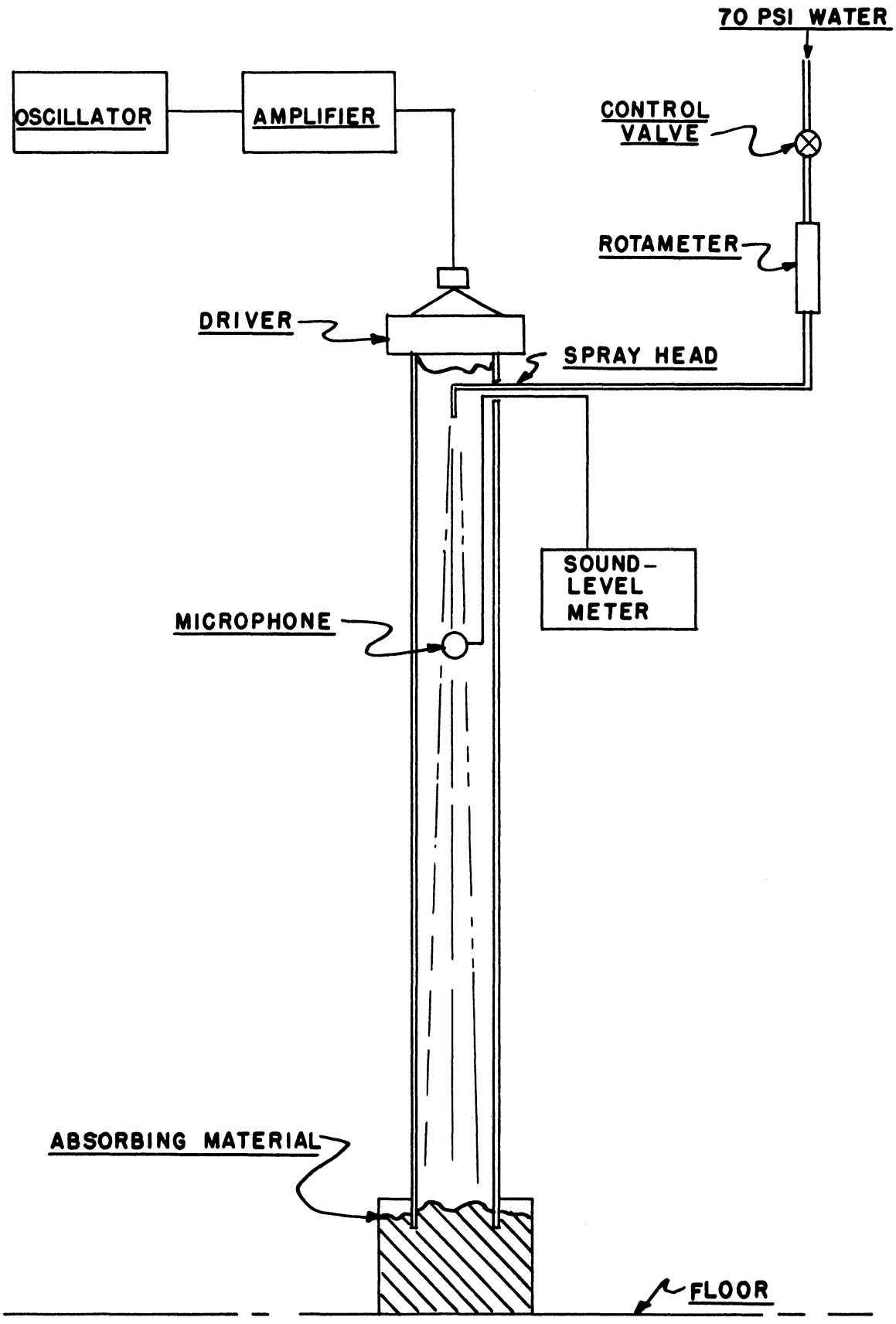


Fig. 14. Apparatus for vertical measurement of sound attenuation.

These conditions when applied to the Sewell equation (see below) give an attenuation of 0.42 decibels for the 15-foot tube.

It is to be noted that the experimental curve for attenuation in the horizontal test setup (Fig. 15) gives an attenuation factor at 300 cycles, much greater than that which was calculated. The experimental attenuation is 4 decibels, while the calculated attenuation is 0.42 decibels. This discrepancy is chargeable to several factors. For one thing, the closest reliable reading which could be made with the sound line meter, considering the method of terminating the tube, was about ± 2 decibels. Also no weighing factor was applied to the drop size taken for calculation. Since there are many drops smaller than the 50-micron median size, and the smallest drops are especially effective for attenuation, it is apparent that the calculated attenuation could be increased on this basis. In addition, the calculated water-air ratio was based on a nozzle velocity of 100 feet per second. This is reduced on striking the air in the tube with the result that the effective water-air ratio is increased. This would further increase the calculated attenuation.

Altogether it appears that when all known factors are considered, there is a reasonable agreement between the experiment and analysis. In this case, the analysis tends to give a conservative result, not because of the theory leading to the analysis, but because of the manner in which the analytical conditions were chosen.

ATTENUATION OF SOUND IN FOG

Sewell* in 1910 derived some equations for calculating the attenuation of sound in a viscous atmosphere containing in suspension cylindrical and spherical obstacles. His equation for the attenuation of sound in an aerosol, in which the density of the suspended spherical particles is large compared to the density of the air, is

$$\alpha = \frac{9}{2}\,\frac{V_p}{c}\left[\frac{\eta}{\rho R^2} + \frac{\left(\frac{\omega\eta}{2\rho}\right)^{1/2}}{R}\right] ,$$

where:

α = attenuation in decibles per centimeter owing to suspended particles,

V_p = volume of the suspended particles per cubic centimeter (V_p is dimensionless; it is the ratio of the volume of the particles

*C. J. T. Sewell, "The Extinction of Sound in a Viscous Atmosphere by Small Obstacles of Cylindrical and Spherical Form", Phil Trans Roy Soc, London (A), p. 210 - 239 (1910).

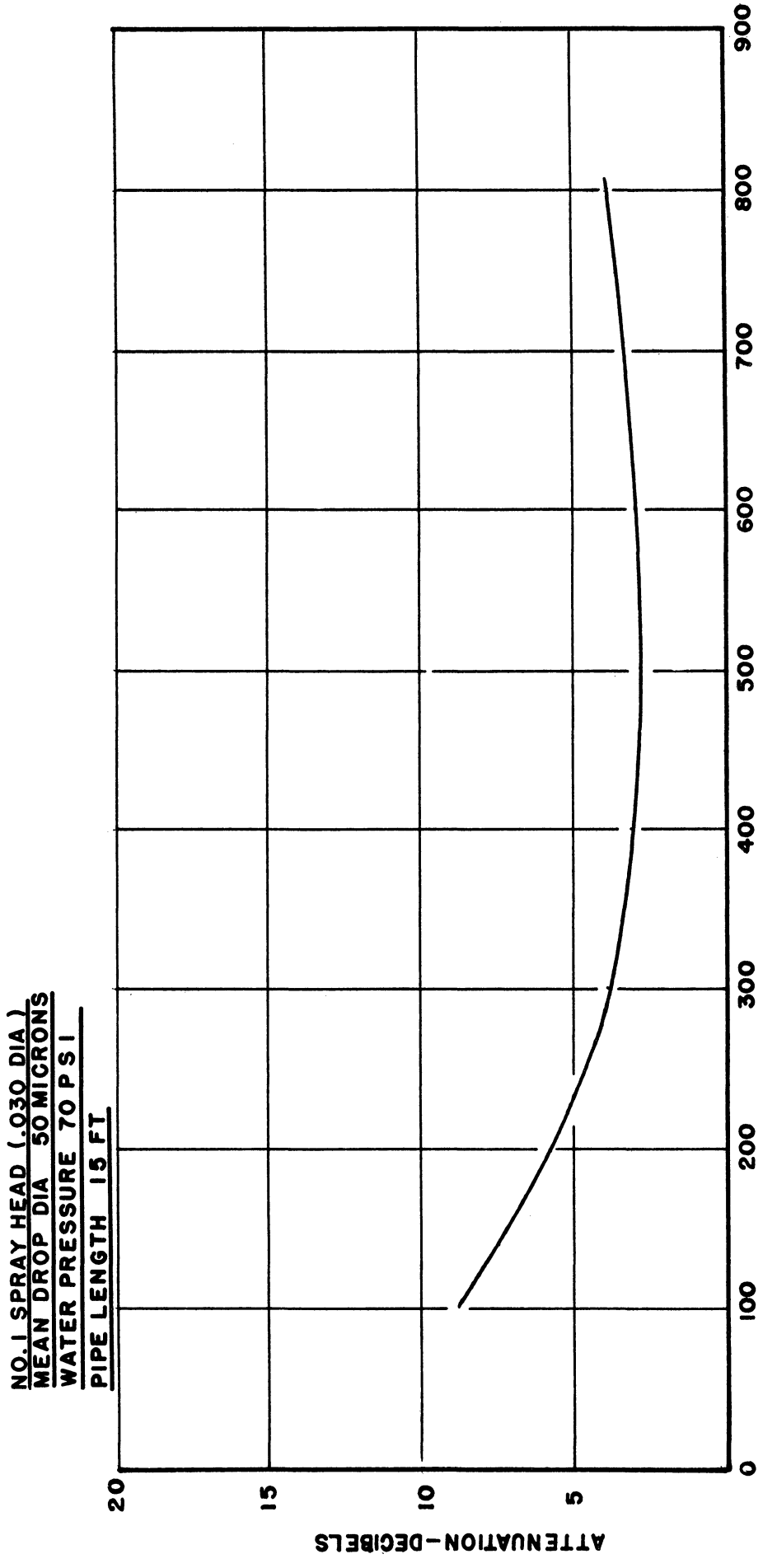


Fig. 15. Attenuation vs frequency, horizontal spray test.

to the volume of the space in which they are suspended.),
c = velocity of sound in air,
η = viscosity coefficient in air,
ρ = density of the air,
R = average radius of particles, and
ω = 2π times the frequency of sound.

Epstein* in 1941 derived and extended Sewell's equations taking into consideration the density and compressibility of the suspended particles. His equation for the attenuation coefficient in an aerosol is

$$\alpha = \frac{9\eta V_p}{2\rho c R^2}(1+d)\,\frac{16a^4(1-d)^2}{16a^4(1+\frac{d}{2})^2 + 72a^3d(1+\frac{d}{2}) + 81d^2(1+2a+2a^2)} ,$$

where:

$$d = \frac{\text{density of air}}{\text{density of particles}} \quad \text{and}$$

$$a^2 = \frac{R^2\omega\rho}{2\eta} ;$$

other quantities are as defined before. In the same notation, Sewell's equation becomes

$$\alpha = \frac{9\eta V_p}{2\rho c R^2}(1+a)$$

Epstein explains that the loss caused by viscosity results from the partial conversion of the incident longitudinal sound wave into a transverse viscous wave which is absorbed in a very short path. Similarly, a longitudinal "thermal" wave is set up when sound is reflected at the boundaries of the particles. This wave, which is associated with the heat conductivity of the air, causes a loss of the same order of magnitude as that caused by the viscous wave. However, this loss associated with the heat conductivity has not been taken into consideration in Epstein's formula. This has been studied by Garvin.** The final attenuation is the sum of the loss due to heat conductivity and the loss obtained from Epstein's equation. The following conditions are assumed to exist in the ramjet addition for purposes of application to the Sewell equation:

*P. S. Epstein, "On the Absorption of Sound Waves in Suspension and Emulsion", Von Karman Anniversary Volume, p. 162, 1941.

**W. W. Garvin, Dissertation, California Institute of Technology.

$$\alpha = \frac{9}{2}\,\frac{V_p}{c}\left[\frac{\eta}{\rho R^2}\;\frac{\left(\frac{\omega\eta}{2\rho}\right)^{1/2}}{R}\right]$$

(a) volume of water spray, 100,000 gal/min
(b) pressure in duct, 1 atmosphere
(c) average temperature in spray-section duct, 600°F
(d) air velocity in duct 300 ft/sec
(e) frequency of pulsation 300 cycles per second
(f) drop diameter, 100 microns = 10
(g) diameter of duct, 16 ft
(h) path length for water droplet, 150 ft

When these conditions are applied to the Sewell equation, the attenuation is calculated to be 0.57 decibels per meter, and for the 150-foot path, a total attenuation of 26 decibels.

In summation, the limited experimental data taken tend to support the Sewell equation. This is in the sense that the known errors in the experimental technique are great enough to bring these results into line with those predicted by the Sewell equation. Since a fire destroyed a refined, experimental setup before any significant data were taken, the only recourse is to use the Sewell equation for computation, with the expectation that the attenuation so computed will be conservative.

SECTION IV. TESTING OF INDIVIDUAL COMPONENTS

The purpose of this section of the report is to show the means by which individual component characteristics are evaluated and to present the results of this evaluation. The primary characteristic of interest is the corner reflection characteristic (β) used in Section II.

The testing of components for the model of the Tullahoma ramjet addition was considered secondary at the inception of the study program. At that time it was hoped that a scale model of the entire system could be constructed and a series of tests made to determine how the exhauster system and the pressure pulsations within it were related. (A sketch and photograph of the scale model of the ramjet addition appear in Figs. 16 and 17.)

It was further assumed that by placing a loud speaker, or other suitable pressure-generating device, at the point which was to be the test cell and introducing a steady pulsation at a constant frequency, it would be possible to measure the sound intensity at the test cell and at the exhauster opening. It was the intention then to use this data to calculate the attenuation of a ducting system. It turned out, however, that it was possible to obtain readings at the exhauster opening that were higher than the measured intensity at the speaker. This is of course readily expected as a result of reverberation and standing waves. This was by no means the end of the difficulty since it was virtually impossible to determine, with any certainty, what sort of a termination a rotating compressor or stationary blading presented to the model of the duct work. The question of a termination plagued the study from the very beginning, since the behavior of the entire ducting system, with respect to the pressure pulsations, is affected by the amount of viscous friction and surge space that is present at the end of the tube. In order to measure the attenuation in a tube carrying pressure waves, it is necessary that reflections from an open end do not travel back up the tube to create standing waves. As a result, the tube must be terminated with a plug of material or a plug and a surge space that will absorb the incident wave. Physically the termination usually exhibits a sloping, wedge-shaped fill with loose granular material or tufts of cotton or glass wool. The proper termination depends also on the frequency since a termination that proved effective at a lower frequency will exhibit properties of reflection at higher frequency. Granted, that with sufficient experiment, it is possible to produce an acceptable termination for a pipe, a driver must further be provided with a duct to transmit the initial wave, the corner or component under test, a tube to transmit the portion of the wave passed, and the nonreflective termination at the end of the final leg of the test assembly (see Fig. 18).

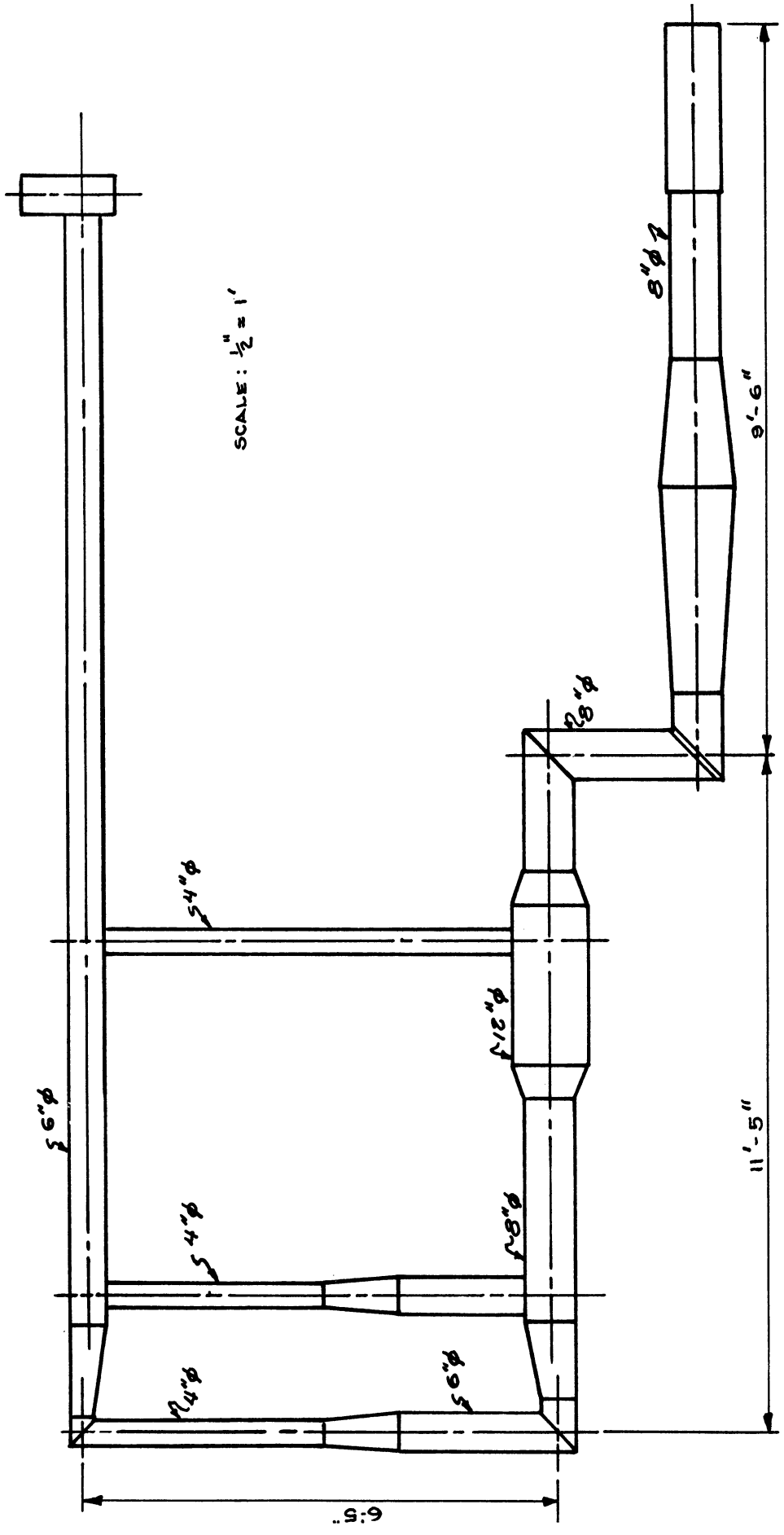


Fig 16. Scale model, ramjet addition (20:1).

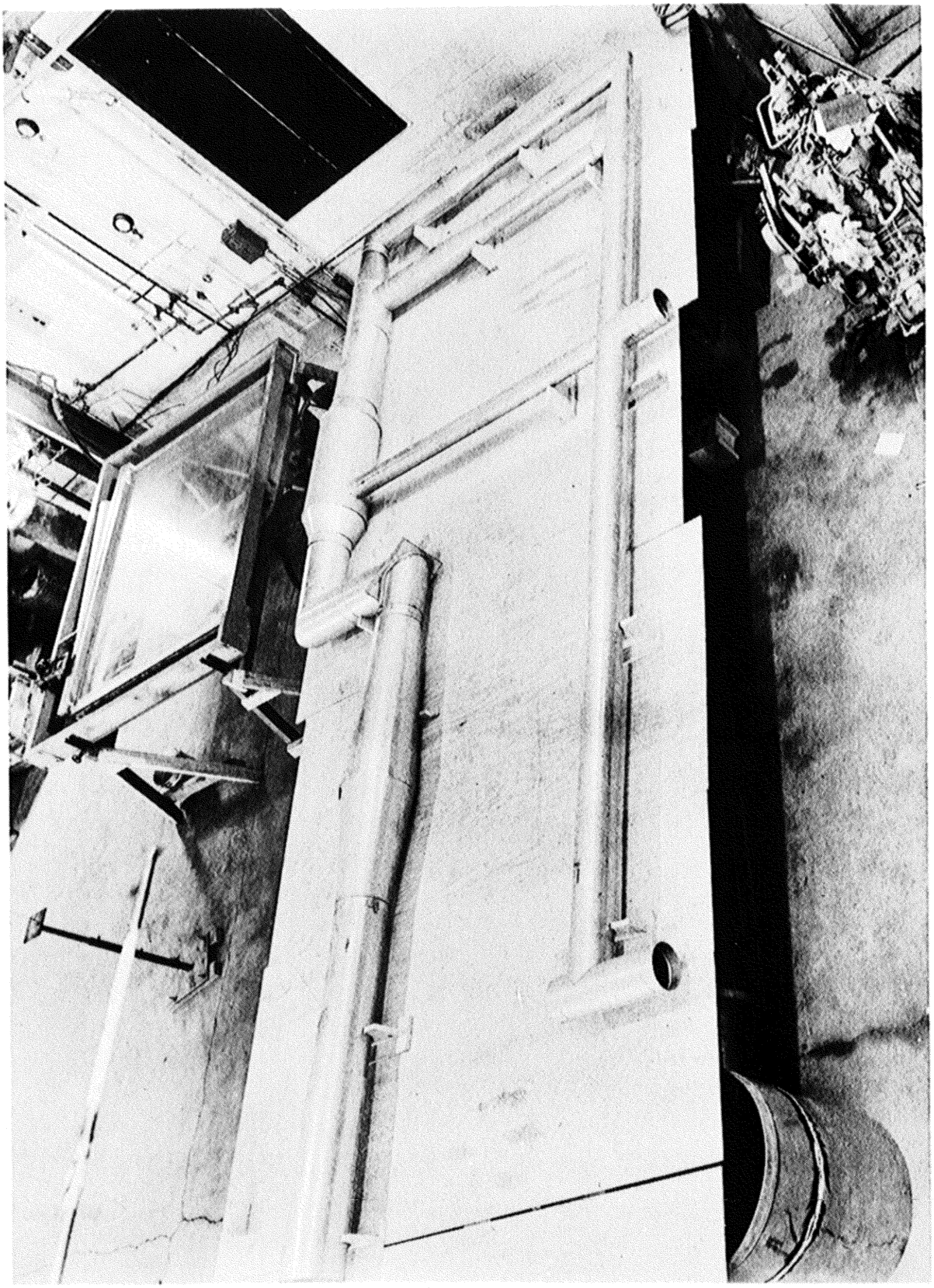


Fig. 17. Photograph of ramjet-addition model.

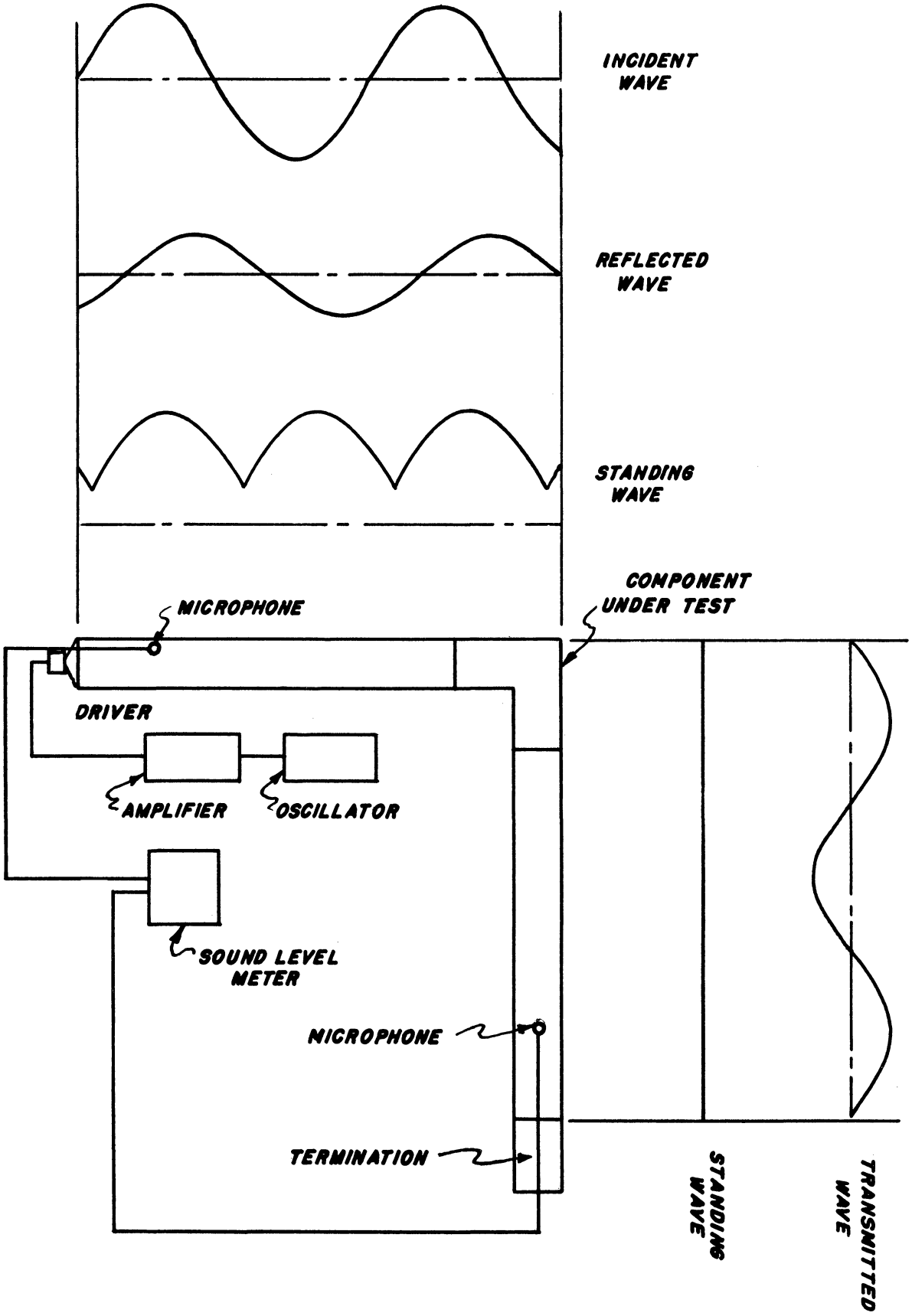


Fig. 18. Experimental apparatus for determining the characteristics of ducting components.

A conventional "first quality" speaker capable of handling the power necessary for the tests was used for a driver, and it was necessary that the speaker be sufficiently large to produce an essentially plane wave in the tube.

The incident wave travels down a connecting tube to the component under test and a portion of the wave returns. The remainder passes through to the termination. The termination must be constructed to successfully absorb all of the impinging wave and still provide access to the equipment for the sampling probe.

The sampling probe was a Rochelle crystal microphone mounted on a wire sled. The sled was attached to a long rod that permitted the operator to move the microphone in and out of the pipe. The loud speaker in the test section received its power input from a variable-frequency audio oscillator coupled to the laboratory power amplifier. Under these conditions the generated sound wave moves down the pipe to the corner or component under test where some of the incident energy is reflected back to the source thereby producing a train of standing waves in the duct. The remainder of the energy passes through the obstruction or around the corner according to the nature of the test. That portion which passes through the device under test moves down to the termination and is dissipated there. The actual situation differs slightly from this ideal. It appears that no termination is completely dissipative so that there is always a small component of reflected wave which results in small standing waves in the terminated leg of the test equipment.

The procedure for the test calls for operating the equipment until the variable frequency oscillator reaches the thermal equilibrium, generating a constant frequency. At this point the sampling probe of the sound-level meter is inserted into the tube. The probe is then inserted by increments of 1 inch and the pressure level recorded after transients due to moving die out. Under these conditions a train of standing waves, which are the sum and difference of the incident and reflected waves, is manifested when the data are recorded in graphical form. A similar procedure is followed in the second leg of the experimental equipment and a similar result is obtained. In this instance, however, if the termination is carefully constructed, the amplitude of the reflected component is sufficiently small to be neglected. The phrase "carefully constructed" may be an oversimplification, since in some instances the termination was reconstructed after the pressure traverse was made in an effort to increase its dissipation. At this point it should be mentioned that at the higher frequency range the interval of probe movement was shortened to 1/2 inch, because the larger increment was too coarse to show all the effects of interests. (The sound-level meter used in these tests is described in Appendix 2.) The pressure level of the pulsations in the ducting are equal to a constant times the antilog of the decibel ratio. These values are plotted in Fig. 19, and are now in a condition where graphical manipulations can be performed. In order to determine the incident wave amplitude, we can add the value of the lower envelope to the upper envelope and divide by two. In effect,

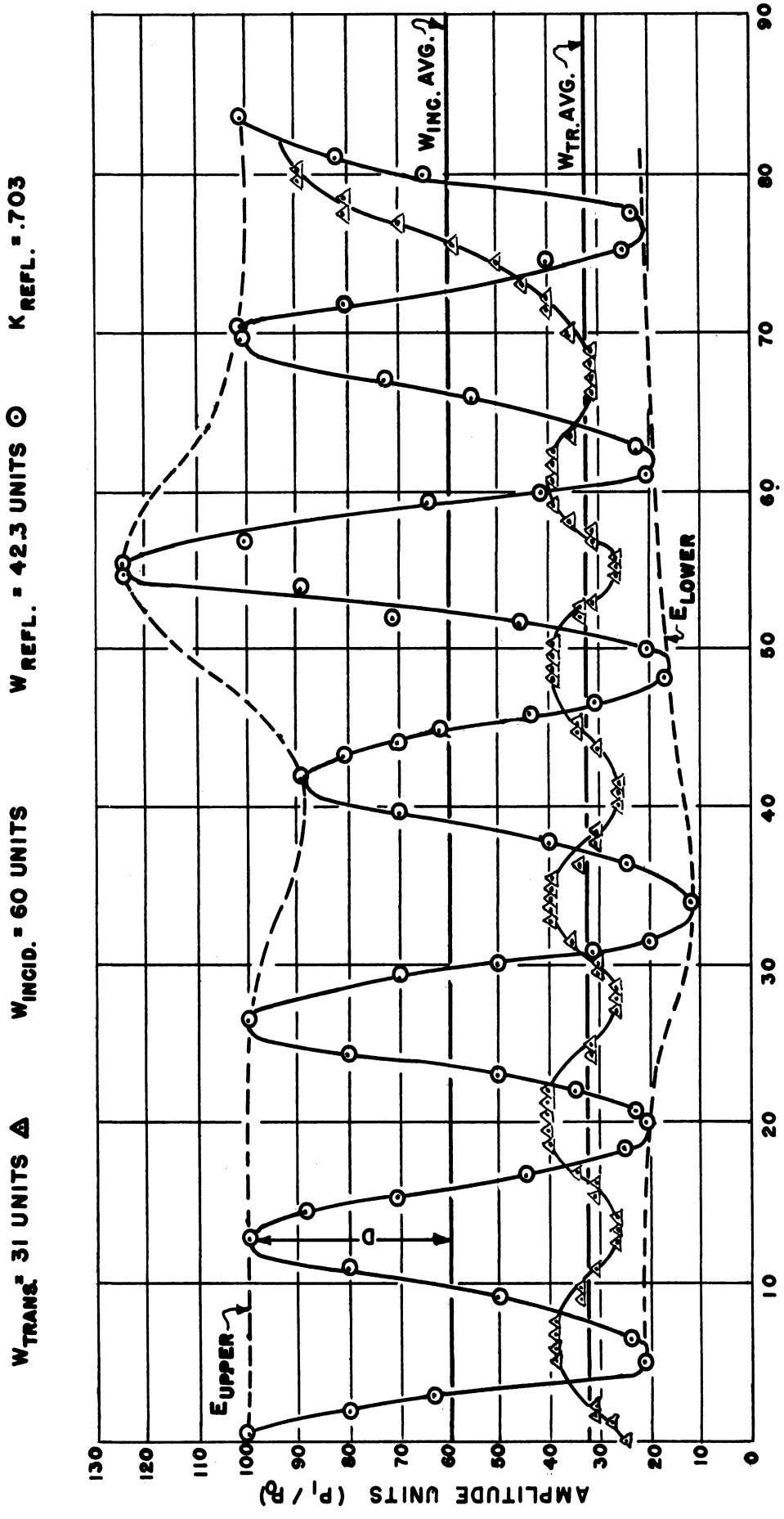


Fig. 19. Standing wave traverse at 500 cycles (square corner without turning vanes).

the mean or average amplitude is found. The value of the reflected wave is the average of the sum of the excursions from the mean line. It is now possible to calculate the amplitude coefficient of reflection for the component at the given frequency. The level on an energy basis is equal to the square of the amplitude level. For example, in Fig. 19, the incident wave has a value of 60 units. The reflected wave has an amplitude of 42.3 units, and the amplitude reflection coefficient is equal to 70.4 percent. An accounting on an energy basis can be made and it is discovered that the incident energy is 3,600 units ($E = KA^2$). The reflected and transmitted energies are 1,790 and 960 units, respectively. The sum of the reflected and transmitted energies is 2,750, which indicates a loss of 850 units and an energy transmission coefficient of 27.8 percent. The reflection coefficient is 50 percent on an energy basis.

After tests at several frequencies it is possible to present data for the amplitude reflection coefficient versus frequency. A sample plot of the operations for finding the wave amplitude appears in Fig. 19. The upper envelope is labeled E-upper, and the lower envelope is labeled E-lower. The excursions are labeled "D" for deviation. In a more precise fashion, the argument can be presented as follows:

> The upper envelope shall be represented by the expression (I+R), which indicates that the upper envelope is the sum of the wave amplitudes. The lower envelope shall be represented in the form (I-R). If these two expressions are now added, the sum is clearly 2I or twice the incident wave, so that it is then logically 1/2(2I) or the average. Secondly, if the expressions (I+R) and (I-R) are subtracted, the result is 2R, and again logically, the reflected wave will be 1/2(2R). The coefficient of reflection is the ratio of R/I.

The mitered corner with the removable guide vanes, that was used in this study, is reproduced for this report as Fig. 20. The guide vanes were designed to slide into the corner from the outside edge, in order to facilitate testing without guide vanes.

Even a cursory examination of Fig. 21 leads to the conclusion that the coefficient of reflection is an increasing quantity with increasing frequency for all the cases tested, with the additional refinement that turning vanes and louvers exhibit similar properties at low frequencies. However, at the midrange frequencies the turning vanes exhibit the properties of reflectors and return considerable proportions of the radiation back to the source. This behavior leads to the conclusion, which is supported by independent theoretical considerations, that at lower frequencies diffraction effects predominate over reflection effects and permit the energy to feed around the corner, whereas at higher frequencies, the diffraction effects are small compared to the dimensions of the system; the phenomena of reflection are accountable for the wave behavior.

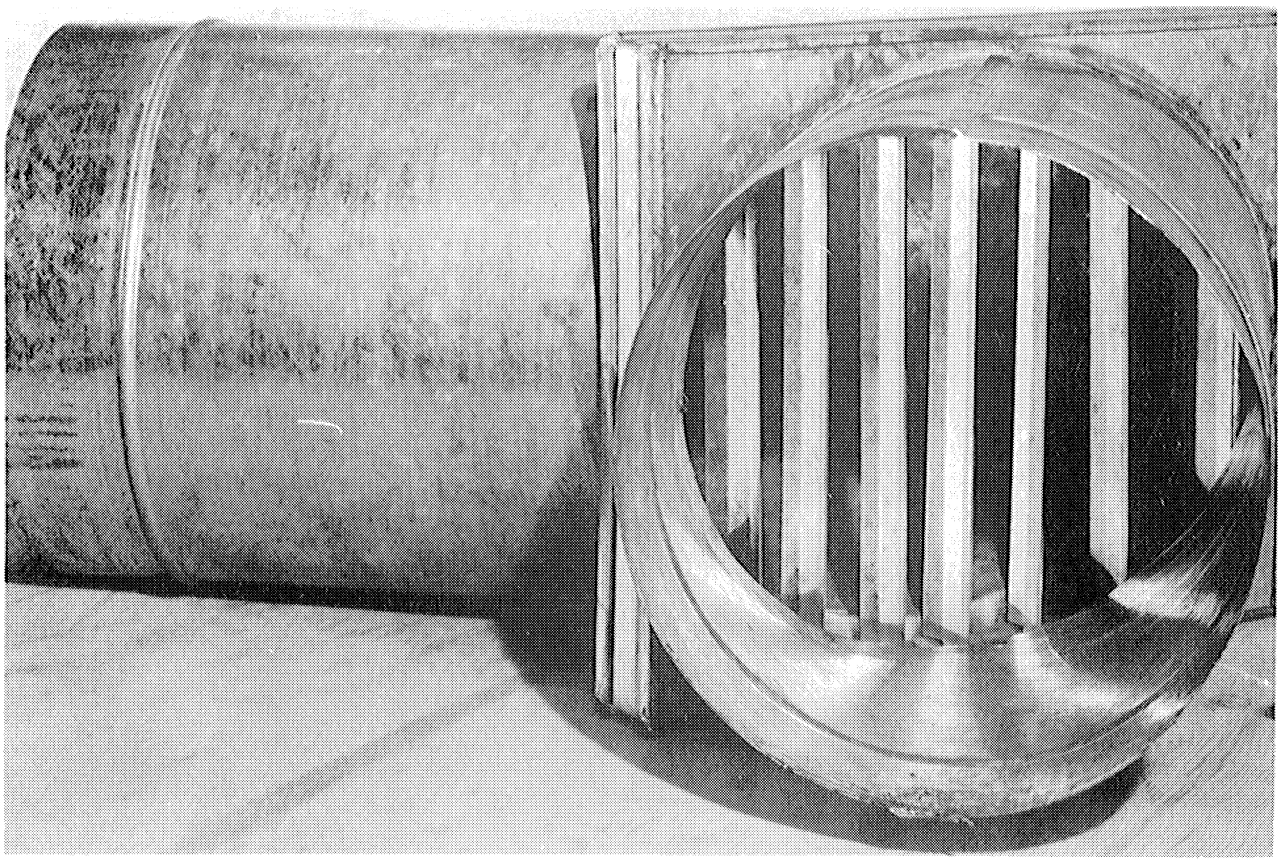


Fig. 20. Mitered corner with turning vanes.

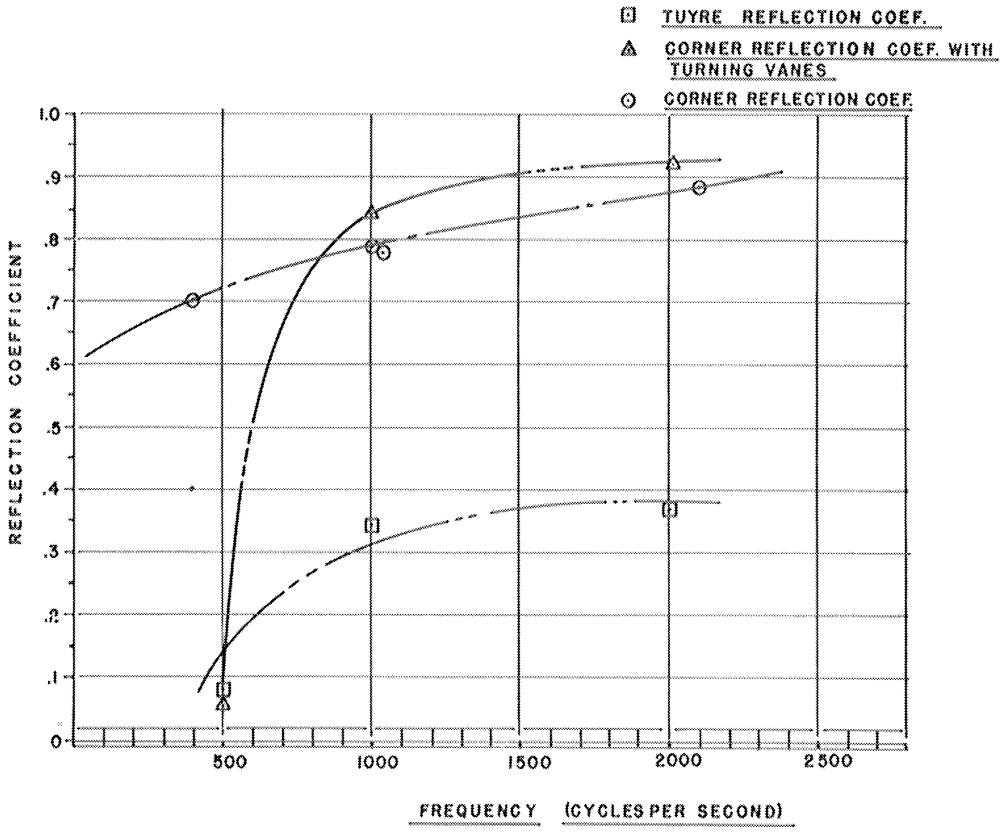


Fig. 21. Reflection coefficient vs frequency.

The phenomena of diffraction provide a ready mechanism for the transfer of low-frequency pulsation around corners. If, for example, a plane wave is permitted to fall on an obstruction, it is found that the pressure pulsations propagate into the geometric shadow. In the case of a plane wave of wavelength 1/8 of 1 meter, the wave will diffract around the obstruction to some extent for a distance of 8 wavelengths along a plane placed a distance of 4 meters from the obstruction and parallel to the wave front. In Fig. 21, the reflection coefficient versus frequency is represented for a square corner, with turning vanes, and for a sample of the steel-tuyère material which is proposed for the centrifix water separator. From Fig. 21, it appears that corner vanes have an effect very much like slots at low frequencies since much of the impinging wave is transmitted as is evidenced by the low value of the reflection coefficient for turning vanes at 500 cycles. At 1,000 cycles, the reflection coefficient appears to be that of a corner without vanes.

It is evident that at a transition frequency between 500 and 1,000 cycles the turning vanes cease to exhibit louver characteristics and behave like a square corner without vanes. The conclusion is that louvers assist the propagation of low-frequency pulsations up to approximately 500 cycles and have no measurable effect on the higher frequencies. There is no intention to convey the impression that the higher frequencies are not affected, but rather that the scale of the experiment made it impossible to detect such effects if they exist.

In summary, corners with and without turning vanes were tested. Sections of tuyère material were also tested. All the components tested show increasing values for the reflection coefficient as the frequency of pulsation is increased (Fig. 21). Losses in all cases were too small to be measured. The transmission coefficients can be taken as the complements of reflection coefficients.

SECTION V. THE STARTING CYCLE

This part of the report is intended to cover the additional work which was done to investigate the starting conditions in the ramjet addition. The main purpose of this work was to examine the system for possible resonant conditions which could adversely affect the exhauster compressors.

During the starting operation, there is apparently no other major source of pressure pulsations than the compressors themselves, and for resonances to develop, it would be necessary for the pulsations to be fed around the return loop or reflected back at the corner of the ducting.

The general statements just made should now be examined in detail in an attempt to place the matter on a more quantitative basis. To begin with, it should be determined in what manner the pulsations are applied to the ducting.

This might be done at a constant energy rate, at a constant potential (pressure variation) or at a constant displacement. The actual manner in which the pulsations are added will in the end depend on the characteristics of the ducting, the characteristics of the compressor, and the manner of coupling between the compressors and ducting. These quantities, and in particular the last two, are so poorly definable from an acoustic basis, that it is probably best to assume a manner in which pulsations are applied and to proceed on that basis. To this end, a constant, potentional pulsation will be considered.

In Fig. 22, an idealized type of feed-around circuit is shown. A closed duct with no sharp bends to cause reflections is shown. Energy at constant potential and frequency is fed in by the driver which is assumed to radiate energy in only one direction.

Under these conditions two important types of resonance can exist. One occurs when the wavelength associated with the pulsations such that an integral number of wavelengths completes the circuit of the duct. The waves always add in phase at the driver, and the vibrational amplitude existing in the air at the driver reaches the steady-state value of $1/1-\alpha$, where unity is the effect produced by the potential alone and α is the propagation constant around the ducting. The other type of resonance exists when an integral number of half waves completes the circuit of the duct.

In this case, the amplitude in the duct reaches the value $1/1+\alpha$, where α is the propagation constant around the ducting. Although this much

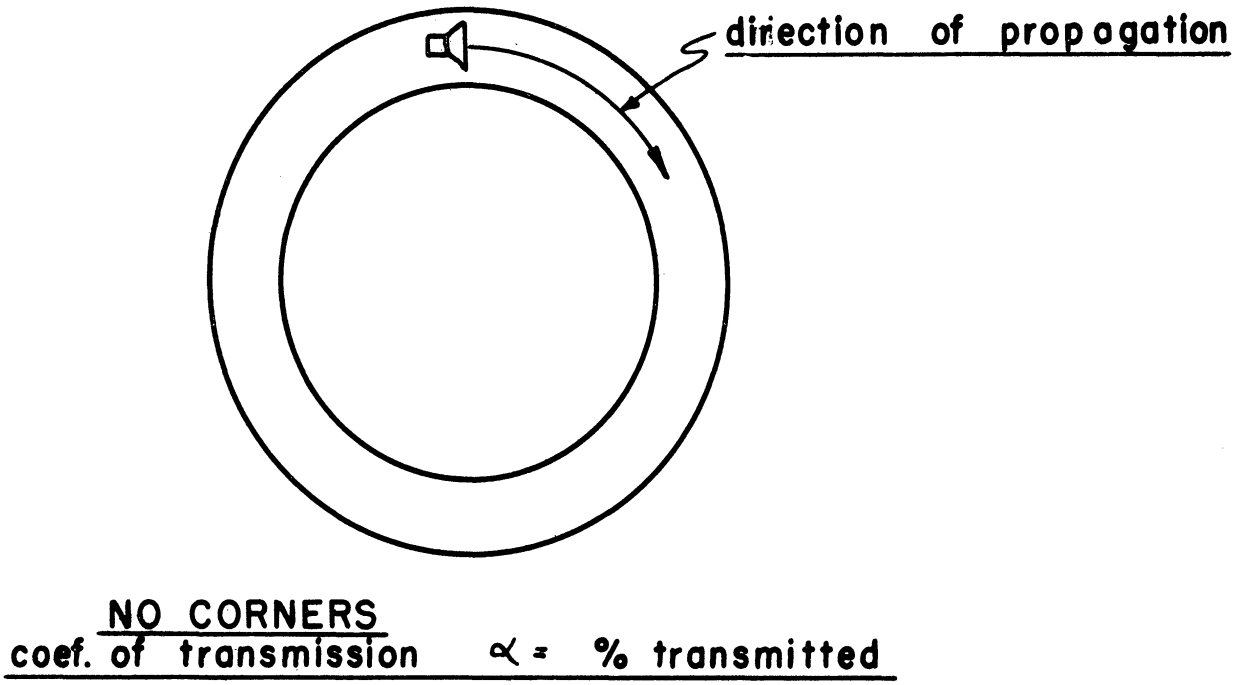


Fig. 22. Idealized, feed-around circuit.

of the analysis rests on simplified concepts, it is already capable of giving useful results. It is seen for example by taking the first case described above, that when the value of α approaches unity, the expression for the air motion approaches infinity.

This is a condition for no losses in the system and the prediction seems reasonable. The second case mentioned leads to the value of 1/2 for the air motion as α approaches unity. Other cases are possible such as when the number of third wavelengths is integral around the duct, but this and succeeding cases fall within the limits already described. A numerical example should be useful.

A case as in Fig. 23 is considered where there are four 90-degree corners in the duct. Experiment and theory indicate that a transmission coefficient of 30 percent for each corner is representative. Taking this value gives: $\alpha = (0.30)^4 = 0.0081$. The limits of the oscillation are then:

$$I_1 = \frac{1}{1 - 0.0081} = 1.01 \quad \text{and}$$

$$I_2 = \frac{1}{1 + 0.0081} = 0.99 \quad .$$

If the corner transmission coefficient is taken as 0.8, the value of α is now

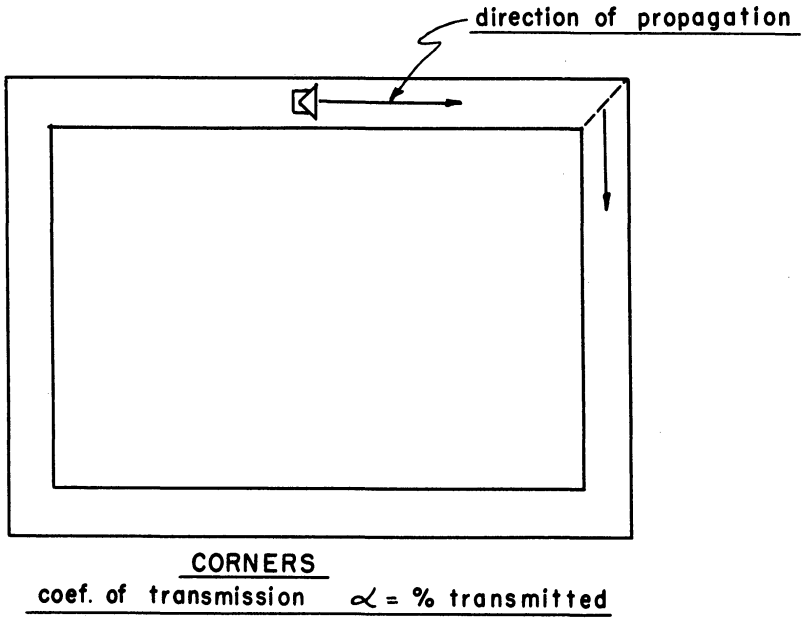


Fig. 23. Idealized, feed-around circuit.

0.4 and the oscillation limits become:

$$I_1 = \frac{1}{1 - 0.4} = 1.67 \quad \text{and}$$

$$I_2 = \frac{1}{1.4} = 0.71 \quad .$$

It is seen that the transmission coefficient must be very nearly unity for each elbow in order that the oscillations due to feed around become serious. The transmission coefficient is generally large (approaching unity) for lengths of straight ducting, but corners, enlargements, and contractions all have transmission coefficients appreciably less than unity.

The preceding analysis shows that the feed-around energy is unlikely to become a serious problem in any complex piece of ducting. An exception to this must be noted, however. This occurs if the compressor itself has the characteristic of amplifying pressure pulsations that are applied to its input. In this case, the effective value of α may approach or exceed unity, and uncontrolled pulsations would result. This characteristic of the compressor should be determined, if possible.

In addition to the feed-around pulsations, there is another way in which resonances may develop in the system. This is by reflections at the corners, and it can be assumed that this type of resonance will exist simultaneously with the feed-around type. As a matter of fact the two types of

resonance should not be separated at all since they are part of the same system, and it is theoretically possible to write a solution for the entire system based on the wave equation if the proper boundary conditions can be described. The inability to do this, however, leads to the approximate approach of considering the resonances as being of two types and then superimposing the solutions.

The ideas to be developed are related to Fig. 24. Again it is assumed that the condition of constant driving force results in an initial wave of unity amplitude traveling away from the driver. At the corner, a portion β of the incident wave is reflected back toward the driver and to the preceding corner. Here the reflection coefficient is β also.

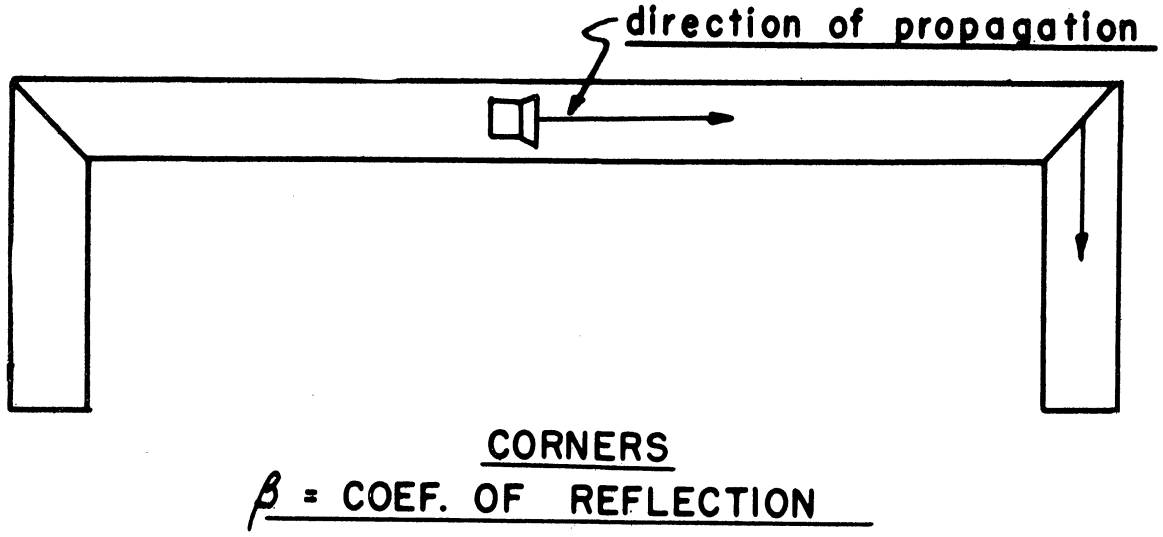


Fig. 24. Idealized, corner-reflection coefficient.

Under conditions of wavelength more restrictive than for the feed-around case (the number of wavelengths must be integral in both the section preceding and the section following the driver), a similar result applies. The motion at the driving unit builds up to the value

$$I_1 = \frac{1}{1 - \beta} \quad .$$

For similar conditions based on half wavelengths, the limit

$$I_2 = \frac{1}{1 + \beta}$$

applies.

The major difference from the feed-around case (aside from the greater

limitation on wavelength) is that the reflection coefficient of a single corner is the significant factor rather than the transmission coefficient of the entire circuit. The transmission coefficient for a single corner has been taken as 50 percent. If the reflection coefficient is also taken to be 50 percent, the value of β is 0.50.

Therefore,

$$I_1 = \frac{1}{1 - 0.50} = 2.0 \quad \text{and}$$

$$I_2 = \frac{1}{1.50} = 0.67 \quad .$$

If β is taken at 0.90, $I_1 = 10.0$ and $I_2 = 0.91$.

It is apparent from the foregoing consideration that considerably larger pulsations may build up due to corner reflection than due to feed around.

When a spectrum of frequencies is considered, it is possible that for certain frequencies, the conditions for integral wavelengths will be met simultaneously for the reflection circuit and for the feed-around circuit. Under these conditions, the greatest pulsations are to be expected, but it is certain that the condition will be realized at fewer frequencies than for the feed around or for the reflection alone.

Another factor is of importance in the analysis of the system. It may be shown that the ratio of the pulsation wavelength to the duct diameter (or other characteristic dimension) is a determining factor in the transmission characteristics of a corner. Without enlarging on this matter, it may be said that for relatively long wavelengths, the laws of refraction hold; and for relatively short wavelengths, the laws of reflection hold.

Thus, with the simple 90-degree mitered bend, it would be expected that the very high frequencies would be transmitted very little. Larger transmission coefficients for the lower frequencies would be expected. Experiment confirms this prediction.

The application of the previous idea to the analysis of the system leads to values for β that are a function of frequency. In other words, at the high frequencies, it is expected that the reflection circuit is predominate, while at the lower frequencies the feed around is dominant. The actual frequency traverses seem to support this theory. At the lower frequencies, the pulsations are not large due to the small value of the transmission coefficient α; there is an occasional peak due apparently to the simultaneous conjunction of the feed-around and the reflection effects. At the higher frequencies, the peaks are more frequent and of larger variation; this apparently is

due to the large value of β.

Another acoustical factor should be introduced now. The foregoing analysis has been based on the assumption of plane waves in the system. If the wavelength becomes smaller than the duct diameter, then the assumption of plane waves no longer holds. Under these conditions, the foregoing analysis has no meaning. In effect, the system becomes so random (in a sense) that it is practically impossible for there to ever be a large simultaneous reinforcement of waves at any one place in the ducting. The frequency traverse indicates this effect, for at the highest frequencies tested, the pulsation peaks tend to drop off again.

The following points should be emphasized in summation. The feed-around circuit appears to offer no problem from a resonant standpoint, unless it can be shown that the compressor possesses definite pressure-amplification characteristics. As a matter of fact, owing to the tremendous mass of the compressor rotating parts, the only source of difficulty from either type of acoustical circuit mentioned earlier could not come from external causes, but must be inherent in the characteristics of the compressor itself.

SECTION VI. APPENDICES

Appendix 1. Blade Vibrations

One of the important considerations in the study of the exhauster system is the level of vibration that may develop in the compressor blading. This is related to the spring constant of the blade, the logarithmic damping decrement, the frequency of vibration, and the power input.

The natural resonant frequency of the blade is the most logical frequency to consider since the blade is not involved with reactive power and is most susceptible to the driving forces at this frequency.

Let x be the displacement of the blade from the neutral position taken in the direction in which the spring constant is measured. The potential energy in the spring for any position of displacement x is then:

$$\text{p.e.} = \frac{k\,x^2}{24} \text{ ft-lb} \quad , \tag{1}$$

where:

x = tip displacement in inches from neutral position and
k* = spring constant, lb/in.

The change in p.e. between any two positions x_1 and x_2 is given by

$$\Delta\text{p.e.} = \frac{k}{24}\left(x_1^2 - x_2^2\right) \quad .$$

If the extreme position of the blade tip on successive cycles of vibration are considered, then the logarithmic decrement conveniently relates these two quantities as follows:

$$x_2 = \frac{x_1}{c^{\text{l.d.}}} \quad \text{and} \tag{2}$$

$$\Delta\text{p.e. per cycle} = \frac{k}{24}\,x_1^2\left(1 - \frac{1}{c^{2\ \text{l.d.}}}\right) \quad . \tag{3}$$

*Value taken from data supplied by the blade manufacturer, The Allis Chalmers Company, Milwaukee, Wisconsin.

$$\text{Power} = \frac{kfx^2}{24}\left(1 - \frac{1}{c^2\ 1.d.}\right) \text{ ft lb/sec} \quad . \tag{4}$$

where:

f = frequency of vibration cycles per second and
l.d. = logarithmic decrement of blade vibration.

The power as defined above, represents the average power which must be continuously supplied to the blade to maintain it in a state of oscillation of maximum amplitude x inches.

It is permissible to drop the subscripts from the x's because the second value is always related to the first by the logarithmic decrement, l.d. The first value of x may be picked arbitrarily, eliminating the need for the subscript.

The power supplied to the blade to maintain oscillation may be expressed in horsepower as follows:

$$hp = \frac{kfx^2}{13{,}200}\left(1 - \frac{1}{c^2\ 1.d.}\right) . \tag{5}$$

This relation applied to the guide vanes gives:

$$x^2 = \frac{(18.8)(13{,}200)}{(3{,}470)(99)(0.30)} = 2.01 \text{ and} \tag{6}$$

$$x = 1.41 \text{ in.}$$

Applied to the first-stage rotor blades the results are: $x^2 = 3.3$ and $x = 1.82$ inches.

Appendix 2. The Sound-Level Meter

The American-type sound-level meter used in making the acoustical measurements described in this report is defined to measure the sound level in decibels. Judging from the construction of this device, it is apparent that what is actually measured is the sound pressure. The sound pressure is always related to the acoustical power because the characteristics of the air (density, temperature, etc.) where the measurements are made are usually fairly constant. It is only in the case where the medium always has constant characteristics that the pressure level can be related to the power level. This is analogous to the electrical case where two voltages can be related on a decibel scale only if they are referred to the same load. The fundamental reason for this rests with the definition of the decibel which, strictly speaking, relates only power ratios. It is apparent, however, that two different voltages working into the same load give rise to power inputs which are related to each other by a function of the voltage ratios. It is thus possible to relate voltages on a decibel scale under certain prescribed conditions. The same, of course, applies to the relation between sound pressure and sound power. The sound pressure as mentioned before may be related on a decibel scale only as long as the characteristics of the air are constant. If this condition does not exist, then correction factors must be used.

Another point of importance in the discussion of the meter is the relation between the power ratio and the pressure ratio. Owing to the squared term which always relates pressure (or voltage) and power, the decibel ratio for a given pressure pulsation is twice that which goes with the accompanying power. It is not clear whether the American-type meter takes this matter into account or not. The meter may simply measure the tenfold logarithm of the pressure ratio. This could, with some logic, be considered a decibel ratio. In order to be strictly accurate the meter should read the twentyfold logarithm of the pressure. Actually when the meter is being used as a comparative device, the concepts above are not of great importance.

Appendix 3. Use of the Water Table

It was anticipated at the beginning of the study of the exhauster system that the water table would play an important part in this work. Experience elsewhere has shown the water table to be generally useful and quite flexible in certain types of flow studies. Unfortunately, the table did not prove itself to be of any great use in the studies made here. This is not necessarily an inherent fault of the water table. It turned out that the degree of refinement and precision which would have to be built into the table in order for it to accomplish the assigned task could not be attained on a project of this size and duration.

The primary application of the water table was to be the determination of reflection and transmission coefficient for components of the ducting system. This was to be done by studying the diffraction patterns caused by the action of plane-front water waves on two-dimensional models of the ducting components.

Three main problems had to be solved in order to successfully complete the work. A way of generating and maintaining plane waves had to be developed; the effects of the boundary of the water table on the wave patterns had to be eliminated, and a means of recording the diffraction pattern had to be provided. The method for recording the data was provided satisfactorily by the arrangement shown in Fig. 25. This arrangement provided a small, brilliant source of light which was projected upward through the water table onto a cloth screen. By adjusting the height of this screen above the water to an optimum value, the wave pattern in the water would be shown very clearly. The screen was then photographed from above using a conventional camera. Except for a certain amount of distortion caused by the relative positions between the light source, the screen, and the water waves, this system worked very well.

The elimination of reflected waves from the boundaries of the table was not accomplished completely. The placing of a sloping ramp of galvanized screen wire around the edge of the table was the most effective procedure tried, but this was not completely effective. The placing of several screens in series would probably serve adequately for eliminating reflections.

The most difficult technique about the water table is to generate and maintain plane waves on the table. A slight difference in the amplitude of the generated wave will change its velocity so that waves, even though generated-plane, will tend to become curved.

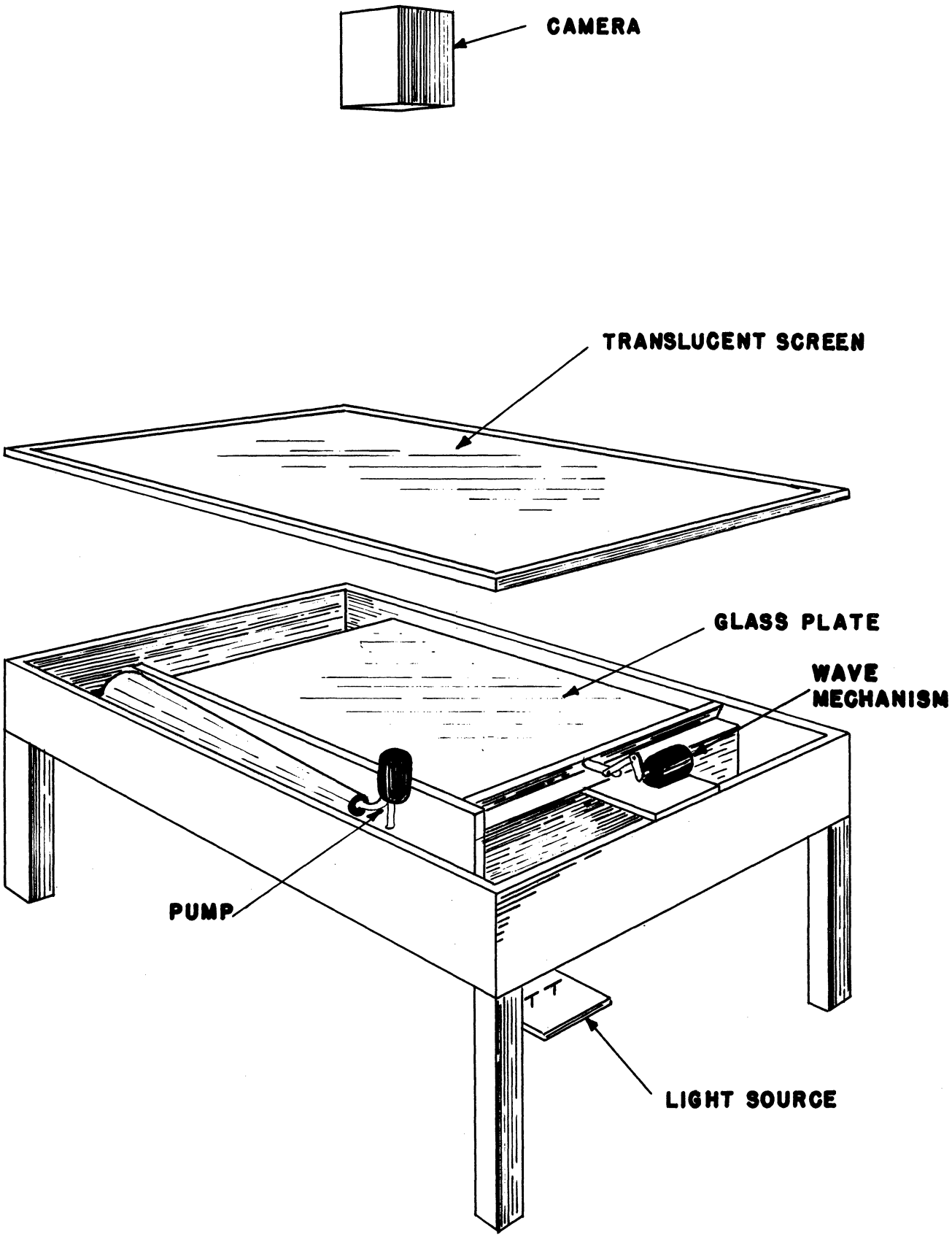


Fig. 25. Water table assembled for wave study.

This difference in wave amplitude can result from a very slight bending of the paddle bar as it rises and falls in the water. Furthermore, unless the water has a uniform depth, the velocity of the waves will not be constant. The slight sag in the glass plate due to the water load is enough to introduce this factor. The importance of maintaining plane waves comes from the necessity of evaluating the results of the work on the table. The diffraction patterns from simple arrangements can be predicted rather easily from geometric considerations, but unless these results can be duplicated on the table, there is no way of knowing whether other results obtained on the table are of any value.

In summation, it appears that a water table constructed with considerable precision, where the expense was not a factor, could be useful in wave-diffraction studies, but anything less than this will not produce the desired results.

Appendix 4. Diffraction and the Frensel Integral

In the body of the report, frequent reference is made to diffraction and diffraction phenomena, and it is therefore desirable that some discussion of diffraction appear in the report. No attempt is made to be particularly rigorous and the following discussion should be viewed as a short condensation of the pertinent aspects of phenomena and theory. The essence of the diffraction theory is based on the work attributed to Frensel as it appears in An Introduction to Acoustics by Robert H. Randall.*

In order to explain the derivation of the Frensel integrals, Fig. 26 is considered. The line B-B' is a line parallel to the advancing wave front. The sound pressure at this plane may be described by the relation

$$p_f = (p_m)_f \cos 2\pi \frac{c}{x} t \quad , \tag{7}$$

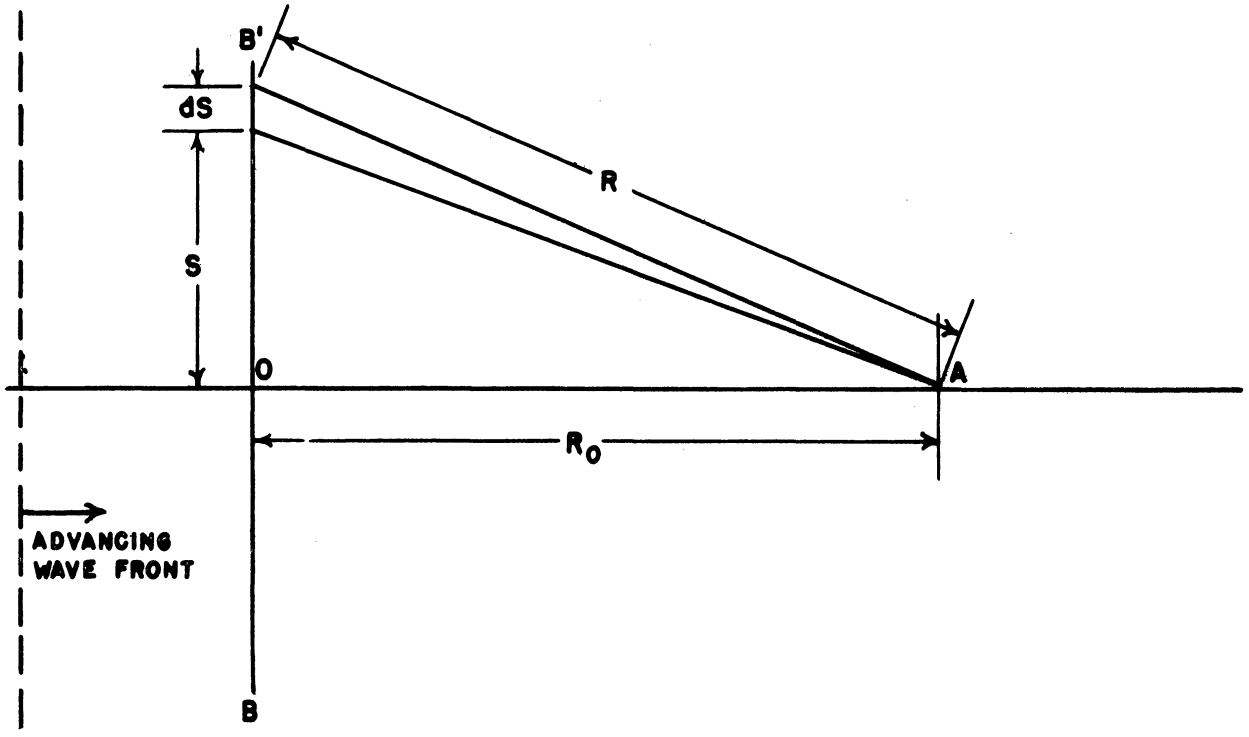


Fig. 26. Geometrical construction for diffraction analysis.

*Robert H. Randall, An Introduction to Acoustics, Addison-Wesley Press, Inc., Cambridge, Massachusetts, 1951.

where p_f is the instantaneous sound pressure and $(p_m)_f$ is the maximum sound pressure. If we now consider the sound pressure at point "A" caused by the disturbance at B-B' by the interval of the wave "dS", it is possible to represent this pressure by writing:

$$dp_A \propto (p_m)_f \cos\left[\frac{2\pi}{\lambda}(ct-R)\right]dS \quad . \tag{8}$$

(This expression neglects considerations such as the attenuation caused by "A" being oblique to "dS" and the inverse square effect of the changing distance from A to dS.

The distance "R" has an effect on the phase of the pressure at "A" with respect to the pressure at "dS". One other point to consider is the distance "R" in terms of R_o and S. "R" is obviously equal to $(R_o^2 + S^2)^{1/2}$, and if the quantity under the radical is expanded by using the binomial theorem, and neglecting all but the first two terms,

$$R = R_o + \frac{S^2}{2R_o}$$

is obtained. If this result is substituted into Equation 8 above and the result is rearranged and expanded as the cosine of the difference of two angles, the differential pressure then becomes:

$$dp_A \propto (p_m)_f \left[\cos\frac{2\pi}{\lambda}(ct-R_o)\cos\frac{\pi S^2}{\lambda R_o} + \sin\frac{2\pi}{\lambda}(ct-R_o)\sin\frac{\pi S^2}{\lambda R_o}\right]dS \quad . \tag{9}$$

Therefore:

$$p_A = \int dp_A \propto (p_m)_f \left[\cos\frac{2\pi}{\lambda}(ct-R_o)\int\cos\frac{\pi S^2}{\lambda R_o}\,dS + \sin\frac{2\pi}{\lambda}(ct-R_o)\int\sin\frac{\pi S^2}{\lambda R_o}dS\right]. \tag{10}$$

Equation 10 is then the summed pressure at "A" when "A" is exposed to the entire front. It is convenient to make a substitution wherein:

$$\int \cos\frac{\pi S^2}{\lambda R_o}\,dS = n\cos\alpha \quad \text{and} \tag{11}$$

$$\int \sin\frac{\pi S^2}{\lambda R_o}\,dS = n\sin\alpha \quad . \tag{12}$$

As a consequence of this substitution:

$$p_A \propto n\,(p_m)_f \cos\left[\frac{2\pi}{\lambda}(ct-R_o) - \alpha\right] \quad . \tag{13}$$

In this study we are interested in diffraction patterns around edges which in effect cut out portions of the wave front B-B'. Thus, since n^2 is proportional to $p_A{}^2$ maximum, attention should be focused on the solution of the equation:

$$N = \left[\int \cos \frac{\pi S^2}{\lambda R_o}\, dS\right]^2 + \left[\int \sin \frac{\pi S^2}{\lambda R_o}\, dS\right]^2 \quad . \tag{14}$$

Equation 14 provides the means for finding the intensity at a given point. In order to increase the utility of Equation 14 and concurrently to generalize the solution the scale factor

$$V\sqrt{\frac{\lambda R_o}{2}}$$

is introduced which is equal to "S". In this instance λ is the wavelength, and R_o the distance normal to the wave front.

Further simplification yields the result:

$$N^2 = \frac{\lambda R_o}{2}\left[\left(\int \cos \frac{\pi V^2}{2}\, dV\right)^2 + \left(\int \sin \frac{\pi V^2}{2}\, dV\right)\right]^2 \quad . \tag{15}$$

These integrals are called the Frensel Integrals. If we call

$$\int_o^V \cos \frac{\pi V^2}{2}\, dV = \text{"x"} \quad \text{and}$$

$$\int_o^V \sin \frac{\pi V^2}{2}\, dV = \text{"y"} \quad ,$$

we have an expression of the character $n^2 = x^2 + y^2$, and when this function is plotted, a figure known as Cornu's spiral is obtained. For the sake of simplicity, and referring to the literature for more extensive treatment, the case where an obstruction cuts off the wave front and extends far in the other direction is considered. In Fig. 27, a generalized picture of the diffraction phenomena is presented, wherein there is a detectable sound intensity within the geometrical shadow.

In Fig. 27, $\mathring{A}$ represents the steady-state wave strength. The point k represents the edge of the obstruction and 1 and 2, the relative amplitudes

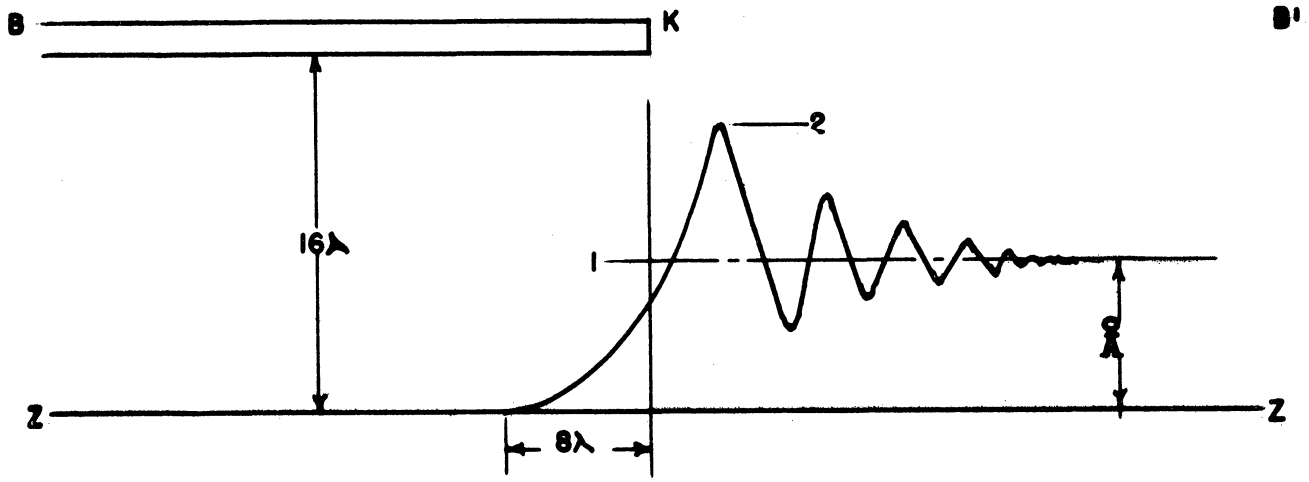


Fig. 27. Wave intensity behind a straight edge.

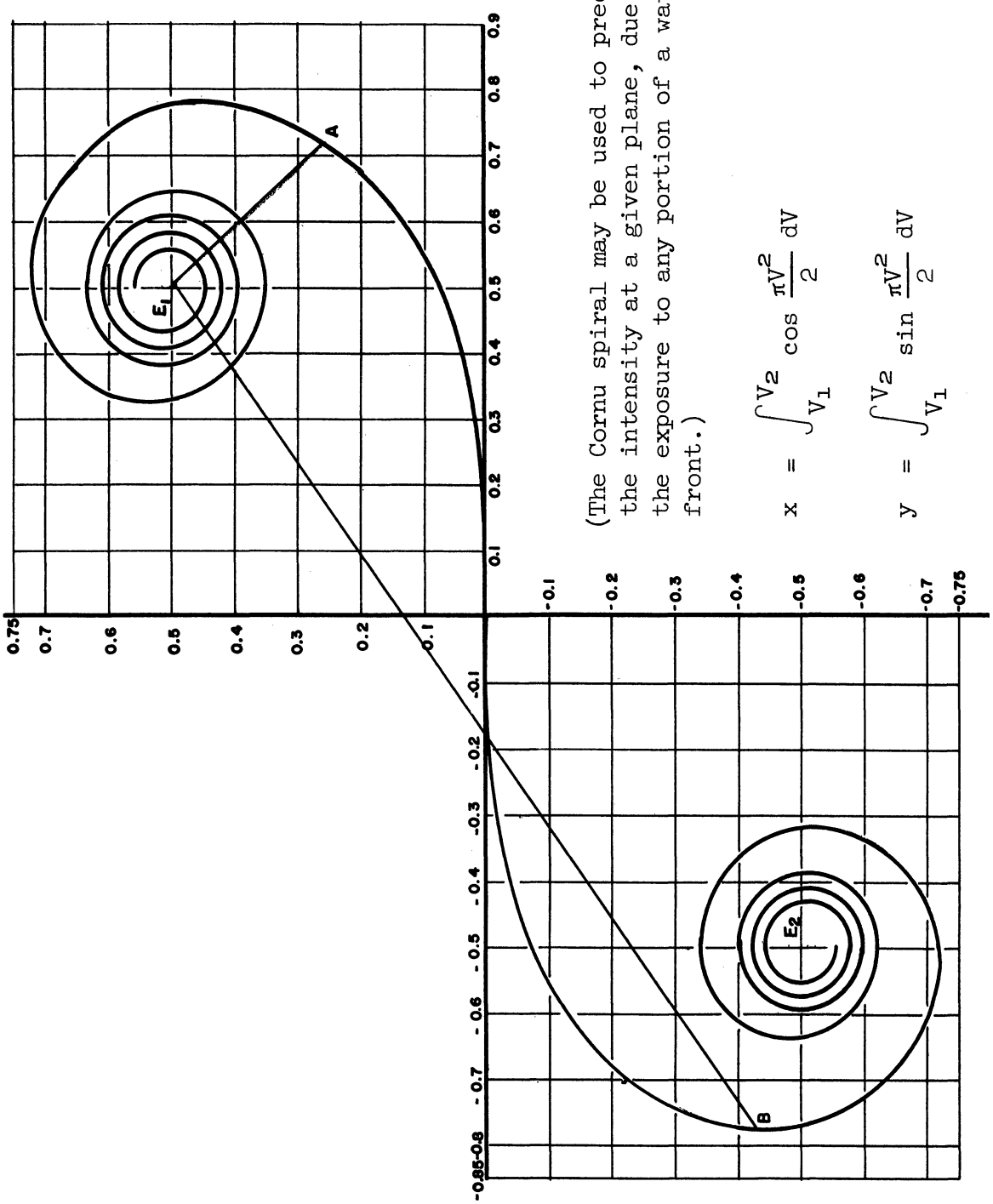
of the wave at points along the plane of observation Z-Z'.

The intensity variation in this instance is of less interest than the fact that the wave front has propagated into the geometrical shadow, since it is this phenomenon that provides the mechanism for low-frequency propagation around bends and square corners. From the diagram it is seen that the wave has an effect for a distance approximately 8 wavelengths into the "shadow".

The use of Fig. 28, Cornu's spiral, makes possible the determination of intensity by graphical means. In Equation 15 the variable "V" represents distance along the spiral in Fig. 28 and for an obstruction that moves out to infinity the variable "V" also approaches infinity; so that for the intensity of any point A, distance S along the plane of observation we take the square of absolute value of the chord between E_1, and a point on the spiral whose distance is

$$S\sqrt{\frac{2}{\lambda R_o}}$$

from the point O which corresponds to the edge of the obstruction. For points within the geometrical shadow, the end of the chord moves along the right-hand portion of the spiral toward point E_1, and the intensity approaches zero asymptotically (i.e., point A). For portions outside of the shadow the point moves along the left-hand portion of the spiral toward E_2, and the intensity is equal to the square of the distance between E_1 and the point on the spiral (i.e., point B). As the point travels around the loop of the spiral, the chord alternately lengthens and shortens producing the intensity variations characteristic of diffraction patterns.



(The Cornu spiral may be used to predict the intensity at a given plane, due to the exposure to any portion of a wave front.)

$$x = \int_{V_1}^{V_2} \cos \frac{\pi V^2}{2} \, dV$$

$$y = \int_{V_1}^{V_2} \sin \frac{\pi V^2}{2} \, dV$$

Fig. 28. Spiral of Cornu.

Appendix 5. List of Symbols

α	=	propagation or transmission coefficient
A or S	=	cross-sectional area of duct, ft^2
β	=	reflection coefficient
c	=	celerity of acoustical pressure, ft/sec
d	=	diameter of duct, ft
ρ	=	average density of air, $slug/ft^3$
f	=	frequency, cycles per second
hp	=	horsepower
I	=	intensity of acoustical power, $ft\text{-}lb/ft^2\text{-}sec$
k	=	spring constant, lb/in.
l.d.	=	logarithmic decrement
λ	=	wavelength, ft or meters
M	=	Mach number
p	=	pressure variation, $lb\text{-}ft^2$
p.e.	=	potential energy, ft-lb
rpm	=	revolutions per minute
t	=	time, sec
x	=	blade displacement, in.

SECTION VII. REFERENCES

1. Beranek, L. L., Acoustical Measurements, John Wiley and Sons, New York, 1949.

2. Crandall, I. B., Theory of Vibrating Systems and Sound, D. Van Nostrand Company, New York, 1926.

3. Lamb, H., Dynamical Theory of Sound, Edward Arnold and Company, London, 1931.

4. Morse, P. M., Vibration and Sound, McGraw-Hill Book Company, New York, 1948.

5. Olson, H., Elements of Acoustical Engineering, D. Van Nostrand Company, New York, 1940.

6. Randall, Robert H., An Introduction to Acoustics, Addison-Wesley Press, Inc., Cambridge, Massachusetts, 1951.

7. Lord Rayleigh, Theory of Sound, Macmillan Company, New York, 1929.

8. Swenson, G. W., Principles of Modern Acoustics, D. Van Nostrand Company, New York, 1953.

9. Wood, A. B., A Textbook of Sound, G. Bell and Sons, London, 1941.